AD NUMBER

AD871424

LIMITATION CHANGES

TO:

Approved for public release; distribution is unlimited.

FROM:

Distribution authorized to U.S. Gov't. agencies and their contractors; Critical Technology; APR 1970. Other requests shall be referred to U.S. Army Aviation Materiel Laboratories , Fort Eustis , Virginia 23604. This document contains export-controlled technical data.

AUTHORITY

USAAMRDL ltr, 23 Jun 1971

AD

USAAVLABS TECHNICAL REPORT 69-96

FEEDBACK CONTROL OF VTOL AIRCRAFT

By

Theodor A. Dukes

April 1970

U. S. ARMY AVIATION MATERIEL LABORATORIES
FORT EUSTIS, VIRGINIA

CONTRACT DA 44-177-AMC-47(T)

DEPARTMENT OF AEROSPACE AND MECHANICAL SCIENCES
PRINCETON UNIVERSITY
PRINCETON, NEW JERSEY

Disclaimers

The findings in this report are not to be construed as an official Department of the Army position unless so designated by other authorized documents.

When Government drawings, specifications, or other data are used for any purpose other than in connection with a definitely related Government procurement operation, the United States Government thereby incurs no responsibility nor any obligation whatsoever; and the fact that the Government may have formulated, furnished, or in any way supplied the said drawings, specifications, or other data is not to be regarded by implication or otherwise as in any manner licensing the holder or any other person or corporation, or conveying any rights or permission, to manufacture, use, or sell any patented invention that may in any way be related thereto.

Disposition Instructions

Destroy this report when no longer needed. Do not return it to the originator.

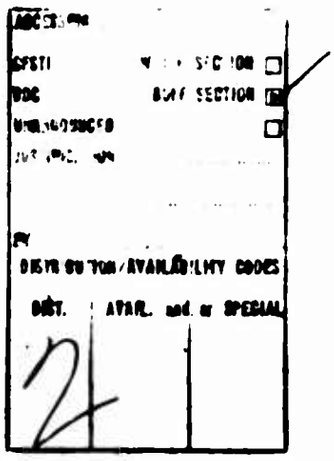

DEPARTMENT OF THE ARMY
HEADQUARTERS US ARMY AVIATION MATERIEL LABORATORIES
FORT EUSTIS VIRGINIA 23604

This report has been reviewed by this Command and is considered to be technically sound. It is published for the exchange of information and the stimulation of ideas.

Task 1F162204A14233
Contract DA 44-177-AMC-47(T)
USAAVLABS Technical Report 69-96
April 1970

FEEDBACK CONTROL OF VTOL AIRCRAFT

By

Theodor A. Dukes

Prepared by

Department of Aerospace and Mechanical Sciences
Princeton University
Princeton, New Jersey

for

U. S. ARMY AVIATION MATERIEL LABORATORIES
FORT EUSTIS, VIRGINIA

SUMMARY

An approximative analysis and discussion is given of the behavior of poles and zeros characterizing the longitudinal dynamics of VTOL aircraft in transition. In feedback design, it is a desirable goal to create a dominant attitude response mode which is separated in frequency and varies little throughout the transition. This investigation has demonstrated that this goal can be achieved at fixed operating points in transition without accurate prior knowledge about the behavior of the stability and control derivatives during transition. In the longitudinal degrees of freedom, pitch attitude and pitch rate feedback were used. In the lateral-directional degrees of freedom, the same goal was achieved by using yaw rate, roll angle, and roll rate feedback. The gains were determined by an approximate procedure.

Longitudinal and lateral-directional experiments were performed with a 0.1 scale model of the XC-142A tilt-wing VTOL aircraft. Pulse responses of the free-flying model are presented. In the longitudinal tests, accelerating and decelerating transitions were flown with the loop closures provided by a small analog computer. The lateral-directional tests were conducted at mid-transition ($i_w = 40^\circ$) at a trim velocity of 18.6 ft/sec. Tests at speeds of 15 ft/sec and 30 ft/sec were conducted representing accelerating and decelerating fixed points in transition, respectively. In these tests, the cross-control gain from differential collective to ailerons was used as a parameter in addition to the feedback gains. The results indicate that a tight yaw rate loop closure makes artificial control uncoupling unnecessary. A pronounced destabilizing effect occurred in the decelerating condition. In the accelerating condition, a more stable spiral mode was apparent.

FOREWORD

This research was performed by the Department of Aerospace and Mechanical Sciences, Princeton University, under the sponsorship of the United States Army Aviation Materiel Laboratories, Contract DA 44-177-AMC-47(T), Task 1F162204A14233. The research was monitored by Mr. Robert P. Smith of the United States Army Aviation Materiel Laboratories. The author wishes to express appreciation to the staff of the Dynamic Model Track, especially Mr. William F. Putman and Mr. John P. Kukon, for its support in the experiments conducted on the XC-142 model.

TABLE OF CONTENTS

LIST OF ILLUSTRATIONS

LIST OF SYMBOLS

B	damping coefficient of desired closed-loop pole pair
C	angular frequency squared of desired closed-loop pole pair
C_L	lift coefficient
DF	degrees of freedom
f.s.	full scale
f( )	function of ( )
g	acceleration due to gravity, ft/sec^2
G	transfer function
H	transfer function of feedback branch
i_w	wing angle, degrees
j	$\sqrt{-1}$
J	moment of inertia
K	factor expressing moment variation due to lift variation; (mass) x (wing lift arm) / (moment of inertia)
$K_{( )}$	feedback gain (subscript indicates feedback variable)
$K_{a\beta}$	cross-control gain from model differential collective to ailerons
K_{ar}	cross-control gain from rudder to roll
$L_v, L_p, L_r, L_{\delta_a}, L_{\delta_r}$	stability and control derivatives, rolling moment
$M_u, M_w, M_q, M_{\delta_e}$	stability and control derivatives, pitching moment
$N_v, N_p, N_r, N_{\delta_a}, N_{\delta_r}, N_{\delta_\beta}$	stability and control derivatives, yawing moment
N	numerator polynomial
$N^{( )}_{( )}$	numerator polynomial of transfer function relating the superscript (output) variable to the subscript (input) variable
r	yaw rate, rad/sec
s	Laplace transform variable
T_{TR}	tail rotor thrust
u_c	carriage velocity

U_o	trim speed, ft/sec
v	side slip velocity, ft/sec
V	volts
VTOL	vertical takeoff and landing (aircraft)
X_u, X_w	stability derivatives, longitudinal force
$Y_v, Y_{\delta_a}, Y_{\delta_r}$	stability and control derivatives, side force
Z_u, Z_w, Z_δ	stability and control derivatives, normal force
$\dot{(\ )}$	differentiation with respect to time
β	collective pitch angle
Δ	characteristic polynomial; denominator of transfer function
$\Delta\ (\ )$	increment of ( )
Δ_β	deviation of collective pitch angle from initial value
δ_a	roll control input
δ_e	pitch control input
δ_f	flap deflection angle
δ_r	yaw control input
δ_β	differential collective propeller pitch angle
ζ	relative damping ratio
θ	pitch attitude, radians
λ	root of characteristic equation
ϕ	roll angle, radians
ψ	yaw angle, radians

SUBSCRIPTS

CL	closed loop
p	port
s	starboard
TR	tail rotor

δ_a	rolling moment control derivative
δ_e	pitching moment control derivative
δ_β	differential collective control derivative
δ_r	yawing moment control derivative
$\theta, \dot{\theta}$	pitch angle and pitch rate feedback
$\phi, \dot{\phi}$	roll angle and roll rate feedback
$\dot{\psi}$	yaw rate feedback

INTRODUCTION

Vertical takeoff and landing aircraft (VTOL) became technically feasible years ago. This family of aircraft is characterized by an essential change in configuration during transition between hover and cruising speed. The effort described in this report is connected with VTOL aircraft in transition utilizing automatic feedback control.

The dynamic characteristics of aircraft are expressed in terms of stability and control derivatives. These can be determined in advance with sufficient accuracy for a conventional fixed-wing aircraft or for a helicopter in hover. In VTOL aircraft configurations, problems arise because of uncertainties in aircraft characteristics and the time-varying nature of the transition dynamics.

It is difficult to predict the exact flow pattern and the forces and moments for all stages of the configuration change. From the feedback designer's point of view, the uncertainties must be considered, but they have a somewhat diminished significance. This is due to the well-known effect that feedback loop closures tend to make the open-loop characteristics disappear as the loop gain is increased. The uncertainties that affect the closed-loop performance of a feedback system were explored in terms of sensitivities of closed-loop dynamics with respect to aircraft parameters.

Stability derivatives are defined only for a fixed configuration and for small deviations from an equilibrium. Because of the acceleration associated with the transition during this maneuver, the aircraft is intentionally not in equilibrium. Utilizing the Princeton Dynamic Model Track and a model of the XC-142 tilt-wing configuration, an experimental investigation of accelerating flight on the closed-loop performance was performed. These experiments and their results are described. The purpose of the investigation was to evaluate the effects of uncertainties and time variation on the closed-loop performance of VTOL aircraft. The approach utilized fixed operating points in transition in the analysis; the effect of time variation was explored experimentally.

TRANSITION

The analytical approach to determine the aircraft dynamics utilized fixed operating points in transition, which means that the configuration was assumed to be fixed and the resulting stability and control derivatives were defined by perturbations about the equilibrium conditions. The behavior of the poles and zeros of the transfer functions was determined. During an actual transition of a VTOL aircraft, as the configuration varies in time, the concepts of "frequency" and "damping" of various "modes" are meaningless and cannot be defined. Nevertheless, for relatively slow transitions, the modes varying in frequency and in damping can provide an approximate shape of the response [1].

The longitudinal dynamics of an airplane in forward flight consist of two modes of motion. In the conventional airplane, these are generally named the short-period and phugoid modes. The former is generally a relatively fast, well-damped oscillation of the aircraft appearing primarily in the attitude response, while the latter is usually a lightly damped, long-period oscillation which proceeds at essentially a constant angle of attack and appears predominantly in the translational response. For the VTOL aircraft in transition, these types of motion are considerably changed. For a tilt-wing VTOL, one of the modes is still referred to as the short-period mode, although the damping will vary from a small negative to a moderate positive value, and the period will change considerably during transition. The other mode is not like the typical phugoid during parts of the transition. Frequently, it will be two real roots: a convergence and a divergence. The time to half amplitude and time to double amplitude, respectively, of these modes vary considerably during the transition.

Fixed operating points in transition define loci of roots of the characteristic equation which describe the root variations between the hovering and the forward flight configuration. As a typical example, in early studies carried out on the longitudinal dynamics of the tilt-wing VHR-447 Tri-Service VTOL aircraft (redesignated the XC-142), values of the roots during conversion were obtained as shown in Figure 1. The separation of roots in frequency (distance from the origin) occurs only approximately halfway through transition and is valid only in the high-speed half of the transition.

The evolution of the roots in the s-plane while tilting the wing forward and retracting the flaps, which corresponds to the takeoff maneuver, will be discussed in this section. The roots follow the same loci in reverse direction when the aircraft converts from forward flight to hover. If these loci were known for any particular configuration, the dynamics of the airplane during transition could be predicted.

The loci of the roots cannot be expected to be uniform for different VTOL designs. Yet it is necessary to state fundamental facts regarding common stability trends and to attempt to establish a mathematical framework as the starting point for the feedback control design.

The influence of the basic lift coefficient slope C_{L_α} is of primary interest. At the higher speed end of the transition, the oscillatory pair of roots can be approximated by the second-order equation (e.g., Reference [2]):

$$\Delta_1(s) = s^2 - (M_q + Z_w)s + M_q Z_w - U_o M_w = 0 \tag{1}$$

Any variation of C_{L_α} would relocate the roots according to the "root locus" defined by the following equation:

$$\Delta_1(s) - \Delta Z_w(s - M_q) = 0 \tag{2}$$

In the low-speed end of the transition, the characteristic roots can be approximated based on the following equation:

$$\Delta_2(s) = (s-X_u)[(s-Z_w)(s^2-M_q s) - gU_o M_w] + gM_u(s-Z_w) = 0 \tag{3}$$

The displacements of the roots following changes in M_u can be estimated by using root locus sketches. The modified characteristic equation with a change ΔM_u in the value of the static stability with velocity is given by Reference [2]:

$$\Delta_2(s) + \Delta M_u\, g(s - Z_w) = 0 \tag{4}$$

There is a strong influence of M_u in shaping the curve of the oscillatory pair of roots at low speeds. This parameter varies over a wide range, according to the configuration selected, flap programming, or geometric displacement of the aerodynamic center with respect to the center of gravity. Positive M_u values are considered to be necessary for achieving acceptable handling qualities, at least until sufficient angle-of-attack stability has built up to produce a stable short-period mode.

The two remaining roots may assume a variety of relative locations through the transition. There are no adequate approximations in terms of stability derivatives which could define the character, oscillatory or aperiodic, of these roots, since approximations are valid only when the roots are firmly separated in frequency. If the static margin is positive, i.e., the constant term of the quartic is negative, these real roots represent a convergence and a divergence.

The vertical translational degree of freedom of a hovering aircraft is dynamically uncoupled from the horizontal degrees of freedom. As the conversion begins, one real root starts to move from the hovering value of Z_w and the other real root moves from its hovering value to the right. Approaching forward flight, these two roots are near the origin and, depending on the sign of the static margin, form a pair of real roots, one positive and the other negative, or a pair of oscillatory phugoid roots. The real parts of the phugoid roots tend to $1/2\ X_u$ as M_u tends to zero.

So far, the general character of the pole movements during conversion has been discussed. For feedback loop closures, the locations of the zeros must also be considered. The first choice of loop closure is an attitude feedback loop, which usually not only stabilizes the hovering roots but also provides a good separation of the short-period roots throughout the conversion.

The approximate values of the two zeros of the pitch-to-stick transfer function during the low-speed end of the transition, where U_oM_w is small, can be determined from

$$s^2 - (Z_w + X_u)\ s + Z_wX_u = 0 \tag{5}$$

which yields

$$\begin{aligned} s_1 &= Z_w \\ s_2 &= X_u \end{aligned} \tag{6}$$

The first zero is coincident with the uncoupled root of the characteristic equation in hovering. The second one is almost equal to zero for a hovering helicopter. For a tilt-wing VTOL, the drag is influenced by small variations of velocity on the effective angle of attack. As the tilt-wing aircraft leaves the hovering condition, the two zeros move steadily along the real axis toward larger negative values.

With increasing velocity of the aircraft, the equation (5) defining the zeros is not valid since the static stability with the angle of attack, U_oM_w, builds up to increasing negative values. Still, a good approximation can be presented as follows:

$$s^2 - \left(Z_w + X_u - \frac{Z_\delta}{M_\delta} M_w\right) s + Z_wX_u - \frac{Z_\delta}{M_\delta} M_wX_u = 0 \tag{7}$$

In arriving at this equation, a negligible value for X_w has been assumed. As a result, the two zeros are given by

$$\begin{aligned} s_1 &= Z_w - \frac{Z_\delta}{M_\delta} M_w \\ s_2 &= X_u \end{aligned} \tag{8}$$

The absolute values of the derivatives Z_w and M_w increase with velocity after some point in mid-transition. The parameter X_u remains substantially limited near the value it attains after the lower speed part of the transition has been performed. As a result $|s_1|$ increases continuously to the end of the transition, and $|s_2|$ remains confined to small values.

Summarizing the general behavior of the poles and zeros of the pitch attitude-to-stick transfer function, a pair of oscillatory poles is dynamically unstable near hover and is moving toward airplane short-period poles after mid-transition. The other poles are at or near the real axis. One of these poles is near the origin throughout the transition; the other moves from the left to the vicinity of the origin. The two zeros are in the vicinity of the origin near hover; as the conversion proceeds toward forward flight, one moves to the left toward increasing negative values. As a result, one pole-zero pair remains near the origin and therefore near the other throughout the transition. The effect of this pole-zero pair on the closed-loop dynamics may be neglected in the first approximation unless the oscillatory pair dips to very low frequencies.

The other pole-zero pair can be considered a first-order equalizer, in series with the varying osicllatory second-order system. This equalizer changes from a lead-lag to a lag-lead configuration. The cg of this pole-zero pair moves opposite to the cg of the oscillatory pair, and the cg of the entire pole-zero configuration moves relatively little throughout the transition as compared to the movements of the individual singularities. The two asymptotes of the root locus plot for an attitude loop closure are parallel to the imaginary axis. The finding that the asymptotes do not vary grossly throughout the conversion is considered favorable, as high-gain attitude loop closures result in predominanat attitude responses that do not vary significantly throughout the transition. Detailed analyses of the longitudinal stability characteristics of tilt-wing VTOL aircraft are found in References [3] and [4].

FEEDBACK DESIGN

Most VTOL aircraft require the application of automatic feedback loops for improving the handling qualities. The stability derivatives at the two end points of the transition, in the hovering and in the airplane configuration, usually can be predicted with reasonably good accuracy. During conversion, insufficiently determined parameters and the time-varying nature of the dynamics lead to considerable deviations among results based on computation, model tests, and full-scale tests.

The fundamental property of feedback is that it tends to diminish the effects of open-loop system variation as the loop gain is increased. If large enough loop gains are used, then, well below the crossover frequency which determines the closed-loop bandwidth, the following well-known approximation holds:

$$G_{CL} = \frac{KG}{1 + KGH} \simeq \frac{1}{H} \tag{9}$$

An efficient feedback system does not have a higher bandwidth than necessary for handling the input spectrum. Much of the operation of the closed-loop system occurs near the crossover frequency, where the gain must "roll off" gradually for stability. The corresponding transient response has a dominant mode with a frequency and damping that affect the handling qualities.

In this study, emphasis was placed on attitude and attitude rate feedback. The controlled or involuntary change in aircraft attitude is a primary source of translational acceleration. Aiding the pilot in the larger bandwidth inner-loop closures permits him to concentrate more on the control of relatively slow translational motions. The following requirements were postulated as the basis for the feedback design for this investigation:

1. There should be a dominant mode in the attitude response to a control input. The period of this mode should be short, and the corresponding roots of the characteristic equation should be separated from those roots which dominate the slower translational response. The short-period requirement implies that the approach of fixed points in transition is justified for the analysis of the attitude loop closures.
2. The frequency and damping of the short-period mode should not vary significantly throughout the transition, so that the dominant attitude response of the aircraft appears approximately the same to the pilot at all times.

PITCH ATTITUDE AND ATTITUDE RATE FEEDBACK

The loci of the poles and zeros of a VTOL aircraft transfer function are known or approximated for the entire transition. Consider the transfer function which relates the pitch response to the control input as shown below.

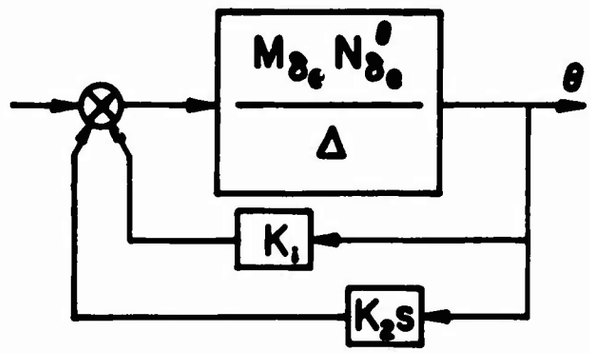

$$\frac{\theta}{\delta_e} = \frac{M_{\delta_e} \; N^{\theta}_{\delta_e}}{\Delta} \tag{10}$$

This transfer function has a second-order numerator, and its denominator is the open-loop characteristic polynomial. With the feedback $(K_1 + K_2 s)\,\theta$, the closed-loop characteristic equation becomes

$$\Delta + (K_1 + K_2 s)\, M_{\delta_e} \; N^{\theta}_{\delta_e} = 0 \tag{11}$$

The coefficients of the quartic are linear functions of K_1 and K_2.

$$s^4 + f_3(K_1)\, s^3 + f_2(K_1, K_2)\, s^2 + f_1(K_1, K_2)\, s + f_0(K_2) = 0$$

Choosing K_1 and K_2, two of the four roots of this equation can be defined. Dividing the polynomial by $s^2 + Bs + C$, the second-order expression corresponding to the desired poles, leaves a remainder which must be identically equal to zero.

$$[f_1 - Bf_2 + (B^2 - C)f_3 - B^3 + 2BC]\, s +$$
$$[f_0 - Cf_2 + BCf_3 - C(B^2 - C)] \equiv 0 \tag{12}$$

This equation yields two linear equations in K_1 and K_2 that can

be solved for the desired gain values. The expressions in these equations depend strongly on the stability derivatives and vary through the transition. With known derivatives, the calculation of the gains is no problem. However, for the usefulness of the approach, the sensitivities of the results to parameter variations must be explored. This is done here on an example in several steps. The data in Reference [2] for the tilt-duct VZ-4 are used for the example (Figure 2). These data are not claimed to be accurate but, rather, to be nominally representative.

Figure 3 shows the zeros and the open-loop and closed-loop poles at hover and at three speeds. The desired short-period poles were prescribed to be at $-3.0 \pm 3.0\,j$. These poles are in the desired location at all speeds because the calculations were made with known derivatives.

Next it was assumed that the derivatives were known only at the end points of the conversion and the following choices were made for the stability derivatives: X_u was to be constant and X_w was to be zero in the entire range; linear interpolations were made for Z_u, Z_w, M_w, and M_q. M_u was considered to be constant.

The assumed functions are shown in Figure 2. The desired gains K_1 and K_2 to produce a dominant short period in $3.0 \pm 3.0\,j$ were calculated with these assumptions, and the results are shown in Figure 4.

Variations of the derivatives due to gross weight, cg location, and accelerating/decelerating flight must also be expected. Therefore, it would be entirely unjustified to use accurate values of K_1 and K_2 as obtained using the choices indicated in Figure 2. Rather, the gain program should be a simple function of the configuration change during conversion. Constant gain programs for desired poles near $-3 \pm 3\,j$ and $-2 \pm 2\,j$ are indicated by dashed lines in Figure 5, and the corresponding closed-loop variations using the known derivative values are shown in Figure 6. The closed-loop short-period mode is not invariant, but its variation through transition is hardly noticeable to the pilot. Figure 6 illustrates that the design principles previously stated can be satisfied with a feedback gain program based on assumptions and approximations.

The desired closed-loop short-period mode is always much closer to the aircraft's own short-period mode than to any of the poles in the hover and mid-transition regimes. Therefore, the feedback gains are always relatively larger in the regions of uncertainties; as a result, the sensitivity of the closed-loop dominant mode to these uncertainties is relatively low. The described design procedure is illustrated here also for the XC-142 model. The experimentally determined stability derivatives of Reference [5] are used as original ("known") information.

The assumed values for the feedback design, instead of the "known" values of Reference [5], are zero for X_w, Z_u, Z_w, and M_w. X_u is taken constant as -0.3, M_u is assumed to decrease linearly from its hover value to zero at the 100 ft/sec point, and M_q is assumed to increase linearly from zero to -.9 at 100 ft/sec. The feedback gain values for closed-loop short-period modes at $-3 \pm 3\,j$ and at $-2 \pm 2\,j$ are shown in Figure 7. Use of the fixed gains indicated in Figure 7 yields the closed-loop dynamics illustrated in Figure 8.

In summary, this section described and illustrated a feedback design principle for the pitch attitude and pitch rate loop closures of two VTOL aircraft in transition. The identical principle can be applied to other aircraft because the insensitivity to the open-loop characteristics due to the application of feedback permits assumptions to be made if the general behavior of the derivatives during transition is known.

LATERAL-DIRECTIONAL FEEDBACK LOOPS

In the lateral-directional degrees of freedom, various loop closures can be considered. In accordance with the requirements stated earlier, separation in frequency of a dominant short-period mode and invariance were considered to be primary goals of the lateral-directional feedback design in this study. As in the longitudinal degrees of freedom, an approximating model was used to determine the feedback parameters; the deviations due to the approximations are illustrated.

The simplified form of the Laplace-transform of the equations of motion is the following:

$$\begin{vmatrix} s-Y_v & -g & U_o \\ -L_v & s^2-sL_p & -L_r \\ -N_v & -sN_p & s-N_r \end{vmatrix} \begin{vmatrix} v \\ \phi \\ r \end{vmatrix} = \begin{vmatrix} Y_{\delta_a} & Y_{\delta_r} \\ L_{\delta_a} & L_{\delta_r} \\ N_{\delta_a} & N_{\delta_r} \end{vmatrix} \begin{vmatrix} \delta_a \\ \delta_r \end{vmatrix} \tag{13}$$

The notation of the controls δ_a and δ_r corresponds to conventional aircraft aileron and rudder controls. In converting VTOL aircraft, in hover and at low speeds, the corresponding angular accelerations are provided in different ways. Differential thrust is used for roll control in most cases. Differential tilting of the thrust vector or separate thrusters are used for directional control. The application of rolling and yawing moments can be separated very well in hover. As the thrust is tilted during conversion, however, any differential

modulation of the thrust provides both a rolling and a yawing moment. Accordingly, besides "phasing out" the hover control mode during conversion, some crossing of controls is usually applied in order to control rolling moments predominantly with δ_a and yawing moments with δ_r throughout. The control derivatives on the right-hand sides of Equation (13) represent the resultant relationships among accelerations and control inputs. Deviations from ideal or assumed uncoupling can have a marked effect on handling. The effect of such deviations on the closed-loop dynamics is of interest especially when multivariable loop closures are applied.

Considering accurate flight path control as an important requirement, translational accelerations with respect to a reference trajectory must be controlled accurately. In hover as well as in coordinated forward flight, the roll attitude provides the dominant control of lateral acceleration with respect to a desired flight path. Therefore, a roll attitude and rate loop closure provides essentially translational acceleration control with respect to a fixed reference path.

As in the longitudinal case, an attempt was made to place a relatively high frequency pair of conjugate complex poles near predetermined nominal locations. The same nominal locations as in the longitudinal case were chosen so as to approximate homogeneity of the short-period responses. This approach in the lateral loop closure design is discussed here as applied to the VZ-4, using the derivative information of Reference [2]. In Figure 9, the given derivatives at the four airspeeds are shown; the approximations used are indicated by dashed lines. In the cases of Y_v, L_p, and N_v, the approximations are straight lines drawn between the two endpoints of what is considered the transition range. L_v and L_{δ_r} are approximated by constants throughout the range; N_p, Y_{δ_a}, and N_{δ_a} are considered zero. In the cases of Y_{δ_r}, N_r, L_{δ_a}, and N_{δ_r}, the curves drawn are the resultants of linear decreases to zero of the hovering values and quadratic increases from zero to the forward flight values. The open-loop poles and the zeros of the ϕ/δ_a transfer function obtained with the original derivatives are shown in Figure 10; those obtained with the approximations are shown in Figure 11. The deviations of the corresponding open-loop poles are minor. The deviations of the zeros are considerable because of the rather sweeping assumptions made about some of the control derivatives. These were made in order to demonstrate the relative insensitivity of the closed-loop fast response to these parameters. In the same two figures are also shown the closed-loop poles when two of them are placed into the $-3 \pm 3j$ points with appropriate K_ϕ, $K_{\dot{\phi}}$ gains. Gains as calculated for the appropriate model are shown in Figure 12, where the choices of constant values for the feedback gains are also indicated. Feedback with these gains is then applied using the original derivatives; the results for two design points, $-3 \pm 3j$ and $-2 \pm 2j$, are shown in Figure 13. This figure shows

the deviations resulting from the fact that fixed gains were chosen based on an approximate model. As can be expected, the application of constant gains throughout results in relatively large deviations at the highest speed where the aircraft itself begins to develop a dominant fast mode in the roll response. During most of the transition, which might be characterized by the lack of such a mode, the constant gain roll attitude and roll rate feedback results in a dominant mode which varies only slightly.

Next, a yaw rate feedback loop is considered. Again, the design is made using the approximate model and then is applied using the original derivatives. First a cross-control from δ_r to δ_a is considered in order to reduce the rolling moments caused by rudder inputs. The ratio $L_{\delta_r}/N_{\delta_r}$ has the following values at the four speeds indicated in Figure 9: 0.278, 0.195, 0.156, and 0.068. With a cross-control gain K_{ar}, the right-hand sides of the lateral equations are modified as follows:

$$\begin{vmatrix} Y_{\delta_a} & Y_{\delta_r} \\ L_{\delta_a} & L_{\delta_r} \\ N_{\delta_a} & N_{\delta_r} \end{vmatrix} \begin{vmatrix} \delta_\ell + K_{ar}\delta_r \\ \delta_r \end{vmatrix} = \begin{vmatrix} Y_{\delta_a} & Y_{\delta_r}+K_{ar}Y_{\delta_a} \\ L_{\delta_a} & L_{\delta_r}+K_{ar}L_{\delta_a} \\ N_{\delta_a} & N_{\delta_r}+K_{ar}N_{\delta_a} \end{vmatrix} \begin{vmatrix} \delta a \\ \delta_r \end{vmatrix} \qquad (14)$$

The rolling moment due to rudder input would be eliminated if the term $L_{\delta_r} + K_{ar} L_{\delta_a}$ was zero. The following values of $K_{ar} = -L_{\delta_r}/L_{\delta_a}$ at the four speeds correspond to this condition: 0.214, 0.250, 0.227, and 0.150. Instead, a constant cross-control gain $K_{ar} = .2$ was chosen which diminished but did not eliminate the rolling moment due to rudder input. The following reduced values of $L_{\delta_r}/N_{\delta_r}$ resulted: 0.019, 0.039, 0.018, and -0.023. With the same K_{ar} value applied using the approximate derivatives, the poles and zeros of the $\dot{\psi}/\delta_r$ transfer function are shown in Figure 14. This figure shows the conjugate complex zeros to be near each other at all speeds. The root locus for the 73 ft/sec speed is also plotted in Figure 14. Based on the root loci, a relatively large but constant $K_{\dot{\psi}}$ feedback gain was chosen, resulting in a fast dominant $\dot{\psi}$ response and bringing the poles close to the zeros.

The poles resulting from the yaw rate loop closures were used as the basis for the roll attitude and rate feedback design. The gains calculated for predetermined locations of two of the closed-loop poles are shown in Figure 15, together with the constant K_ϕ, $K_{\dot{\phi}}$ values chosen.

Finally, the constant K_ϕ, $K_{\dot{\phi}}$ values indicated in Figure 15 were used for roll attitude and rate feedback gains, with the poles of Figure 14 as open-loop poles. The block diagram of the corresponding feedback system is shown in Figure 16. Figure 17 shows the closed-loop poles using a constant cross-control gain $K_{ar} = .2$, a constant yaw rate feedback gain $K_{\dot{\psi}} = 2$, and constant roll angle and rate feedback gains K_ϕ and $K_{\dot{\phi}}$ for $-3 \pm 3j$ as the predetermined fast mode to be approximated. The variation of the oscillatory mode is within a relatively confined area. This illustrates that using the applied loop closures leads to relatively invariant closed-loop dynamics in the transition region, even though the constant gains were determined based on an approximating model. The same principles and method can be applied to the feedback design of other aircraft in transition.

MODEL EXPERIMENTS WITH FEEDBACK

The Princeton University Dynamic Model Track provides a unique capability to test free-flying models at low speeds (Reference [6]). A 0.10 scale dynamically similar model of the XC-142A tilt-wing aircraft has been tested extensively in this facility, and this model was used in the course of an experimental program to explore the closed-loop dynamics with a variety of feedback gains. The model angular degrees of freedom were instrumented with potentiometers and miniature rate gyros to provide the attitude and rate information necessary for the feedback experiments. In addition, a tail rotor support system was installed that allowed measurement of the tail rotor thrust by means of strain gauge instrumentation. The servos used to position the model pitch, roll, and yaw controls have bandwidths of approximately 3 Hz. An eight-amplifier analog computer was used to provide the necessary loop closures and gain adjustments. An additional unit with two servo multipliers was used to provide programs for pitching moment trim and vertical force trim. The computer and the program servo were mounted on the dynamic carriage that follows the model motions. The following model electrical signals were available at the computer:

Wing angle	Roll angle
Pitch angle	Roll rate
Pitch rate	Yaw angle
Vertical error	Yaw rate
Horizontal error rate	Vertical sink rate
Flap position	Lateral error rate

In addition, there were connections to the following actuator servos:

Starboard collective pitch
Port collective pitch
Tail rotor collective pitch
Flap deflection
Wing incidence
Starboard aileron
Port aileron

LONGITUDINAL MODEL EXPERIMENTS

In the first longitudinal test series, both one- and two-degrees-of-freedom (pitching, and pitching + horizontal velocity) runs were made at hover. Trim difficulties and the observation of nonlinear dynamic behavior led to a careful investigation of the tail rotor thrust characteristics. It was established that the tail rotor thrust vs. collective characteristic exhibited a strongly nonlinear shape, as

can be seen in the uncompensated portion of Figure 18. In the region of zero thrust, the slope of the thrust vs. tail rotor pitch curve was approximately 3.6 times smaller than elsewhere. The width of this portion was not negligible; it amounted to 22 percent of the full range. The model trim point under investigation required a tail rotor pitch that was near a rather sharp slope change; previously-observed inconsistencies and nonlinear behavior could be attributed to this slope change characteristic. It was established that the measured nonlinear thrust vs. blade pitch angle was a characteristic of the tail rotor and was not caused by some mechanical inadequacy. The situation was remedied for the purpose of the test series by means of nonlinear compensation in the computer. The characteristic of the amplifier providing the input to the tail rotor collective servo was altered in such a way that the resultant characteristic between the input to that amplifier and the tail rotor thrust appeared quite linear. Figure 18 illustrates the nonlinearity before and after compensation by showing the distortion in tail rotor thrust when a constant amplitude triangular wave input is sweeping through the entire range. A nonlinear behavior of similar character was observed on the full-scale tail rotor in the vicintiy of zero thrust.

Some improvement in the linearity of the thrust vs. pitch characteristic was obtained by "staggering" the blades so that only one blade had near-zero pitch angle at a time. Although this approach improved the linearity of the characteristic, it also made it more difficult to compensate and was therefore abandoned. As the final solution, the nonlinear compensation was combined with a 3-Hz sinusoidal dither with a peak-to-peak amplitude of approximately 3 percent of full scale. This was necessary in order to remove the effect of small-scale nonlinearities which remained even after the nonlinear compensation was applied.

In the course of preparations for three-degrees-of-freedom runs, the need for accurate thrust adjustment became obvious, since a small deviation from vertical equilibrium soon brought the model to the limit of its vertical travel. A vertical velocity integral control was used in the vertical loop with the vertical velocity feedback for stability. A tight vertical loop, however, would have interfered with the three-degrees-of-freedom motion, almost acting as a constraint on the motions. Therefore, the tight vertical loop closure was used in constant-speed portions of the runs only, and before pitch release and the actual transient test. In the standard test procedure, the model was first accelerated by the carriage to the trim speed; then the model was released vertically and horizontally, but not in pitch. During this period, the vertical velocity integrator control established force balance. At the time of pitch release, the vertical loop circuit was interrupted but the integrator maintained the proper value for vertical balance. Immediately after pitch release, the input was applied to the tail rotor.

Various flight conditions were tested at constant speeds as well as in accelerating and decelerating flight. Pitch attitude and rate feedback was used in all tests, and in most cases a pulse input was applied to initiate a transient. The following gain values were obtained by careful calibration:

Pitch attitude	.295 V/deg
Pitch rate	.115 V/(deg/sec)
Control moment (hover)	1.1 ft-lb/V

The moment of inertia was measured as $J = 1.54$ (ft-lb) / (rad/sec^2); the mechanical damping ratio in pitch was determined as $\zeta_{mech} \approx .015$, which is negligible.

The loop gain of the feedback loop closures was calculated as follows:

Pitch attitude loop gain:

$$K'_\theta = [\text{pitch pot calibration}]_{15\ V/rad} \times [\text{computer gain}]_{K_\theta\ V/V} \times [\text{control effectiveness}]_{1.1\ (ft\text{-}lb)/V} \times [1/(\text{inertia})]_{.65\ (rad/sec^2)/(ft\text{-}lb)}$$

Pitch rate loop gain:

$$K'_{\dot\theta} = [\text{rate gyro calibration}]_{6.6\ V/(rad/sec)} \times [\text{computer gain}]_{K_{\dot\theta}\ V/V} \times [\text{control effectiveness}]_{1.1\ (ft\text{-}lb)/V} \times [1/(\text{inertia})]_{.65\ (rad/sec^2)/(ft\text{-}lb)}$$

$$K'_\theta = 10.7\ K_\theta \ ; \qquad K'_{\dot\theta} = 4.7\ K_{\dot\theta}$$

where K_θ, $K_{\dot\theta}$ are the feedback gains as set on the analog computer. The full-scale K'_θ and $K'_{\dot\theta}$ are from Reference [7], $K'_\theta = 31.8$ and $K'_{\dot\theta} = 6.1$.

The corresponding short-period poles are $-3.27 \pm 4.58\ j$. The corresponding scaled response would have a natural frequency of approximately 3 Hz. (For scaling information, see Reference [5].) No useful test data could be obtained from the model at such high frequencies. Therefore, it was decided to consider control gains for model time and to explore gain ranges including and close to low damping. Characteristic longitudinal runs as identified by run numbers are shown in Figures 19 through 25.

Runs 2142, 2146, 2152, and 2158 are two-degrees-of-freedom runs in hover. These runs map the margins in damping. Run 2142 was considered to be a desirable combination of gains for testing in order to be able to detect differences in the response due to parameter variations.

Run 2179 shows the unstable open-loop response in hover. In this run, the tail rotor control was inoperative, so that neither input nor control was applied. The smooth start of the transient is the result of careful trim adjustments.

Run 2192 is one of the first three-degrees-of-freedom runs, near hover, at U_o = 5 ft/sec. Compared with Run 2142, only slightly lower damping can be noticed.

In the course of preparations for transition testing, it was found necessary to provide a vertical loop closure to the propeller pitch angles β_s (s for "starboard") and β_p (p for "port"). For this purpose, two-degrees-of-freedom runs (vertical and horizontal) were made with the model locked in pitch in order to establish the necessary β program. In Run 2207 (Figure 22), the wing rotated from 90° to 50° in 15 seconds., and the flaps traveled 18 degrees from 74° to 56°. A tight vertical loop held altitude in the first half of the run; all collective angles (tail rotor, port, starboard) are shown as deviations $\Delta\beta$ from initial values throughout this report. The range was adjusted always so that the needed travel of blade angles would be within range for the various experiments. This way the shape of the necessary β program was established.

Run 2225 (Figure 23) was the first successful transition in which all controls remained within range. For accurate attitude control, not only was the pitch loop stiffened using K_θ = 5, but also an integral control was added with a gain $K_{\int\theta}$ = 1. In this way, the tight loop closures provided the proper β and β_{TR} time histories for this 16-second (50-second full scale) transition with the flap program shown.

Run 2227 shows an 8-second transition with the same flap program. Notice that no phugoid-like motion can be detected.

In Run 2243, the pitch feedback gain was lowered to K_θ = 1 but the tight vertical loop was maintained. Because of the looser control loop, the β_{TR} input altered the transition noticeably.

For Run 2250, the feedback gains were lowered further to K_θ = .5 and $K_{\dot\theta}$ = 2.5. Figure 24 shows three runs at a fixed point in transition with the model trimmed at a wing angle of 60°. At the beginning of these runs, the model was accelerated to, and released at, 18 ft/sec.

The initially tight loop gains were lowered to the test gains after 3 seconds, just before the input was applied. In Run 2253, the test gains were $K_\theta = .7$ and $K_{\dot{\theta}} = 3.5$. Much better damping than in hover was obtained at this speed, as might be expected. For Run 2254, the gains were lowered by another factor of 2. The low damping of Run 2255 resulted with $K_\theta = .2$ and $K_{\dot{\theta}} = 1$. A tight vertical loop was maintained throughout these runs.

The last three longitudinal runs are shown in Figure 25. Runs 2270, 2273, and 2276 were made under the most difficult test condition: decelerating transition. In Run 2270, the model was released at 29 ft/sec and all loops were tight all the way in order to establish the trim programs for the collective controls. It can be observed that both controls traveled their carefully adjusted full range during this transition.

In Run 2273, the pitch loop gains were lowered after release to $K_\theta = .7$ and $K_{\dot{\theta}} = 3.5$, and then an input was applied; it is clear that the transition was much less under control than with all loops tight. Finally, for Run 2276, the gains were lowered by a factor of 2. A tight vertical loop was maintained throughout the decelerating transition runs.

The test runs shown in Figure 25 indicate that tight pitch loop control must be maintained, especially during the decelerating transition, even with tight altitude control, and even if the vertical degree of freedom is virtually uncoupled.

LATERAL-DIRECTIONAL MODEL EXPERIMENTS

For the lateral-directional model experiments, the XC-142A model was mounted on the "lateral carriage" described in Reference [8]. Prior to the feedback experiments, open loop tests were conducted. The results of these experiments are reported in Reference [9].

The analog computer described earlier was used to provide the loop closures. The voltage calibrations of the model variables yielded the following values:

Roll angle	.22 V/deg
Yaw angle	.12 V/deg
Roll rate	.32 V/deg/sec
Yaw rate	.32 V/deg/sec
Aileron effectiveness	11.6 $deg/sec^2/V$
Differential collective effectiveness	37 $deg/sec^2/V$

Because of the limited time available for the lateral-directional feedback experiments, the scope of this test series had to be somewhat limited. A mid-transition configuration was tested at three steady speeds: at trim speed and at one higher and one lower speed, the latter two being representative of decelerating and accelerating fixed points in transition since in an actual transition the airspeed is always higher or lower, respectively, than the trim speed which corresponds to the wing angle at any instant. The wing and flap angles chosen were $i_w = 40^\circ$ and $\delta_f = 60^\circ$. The three test points were:

	Trim	Decel.	Acc.
Model velocity U_o (ft/sec)	18.6	30.0	15.0
Full-scale velocity (ft/sec)	58.7	94.7	47.3
Collective pitch β (deg)	13.5	10.7	15.4

At this wing angle, a differential collective input causes both rolling and yawing moments. Therefore, a cross-control from the differential collective to the ailerons was employed and the gain of this electronic link was a test variable.

The feedback gains used in the tests were referenced to gain values which corresponded to full-scale feedback gains as obtained from Reference [7]. These values of roll attitude, roll rate, and yaw rate gains and the corresponding model gains calculated with the proper factor are given below:

	$K_\phi L_{\delta_\beta}$ (1/sec^2)	$K_{\dot\phi} L_{\delta_\beta}$ (1/sec)	$K_{\dot\psi} N_{\delta_r}$ (1/sec)
Full scale	3.3	3.3	2.0
Model	33.0	10.4	6.3

The feedback gains used in the model tests were expressed in terms of fractions of these gains and are identified as 1/4 f.s, 1/8 f.s., for example. The high gains which correspond to the full-scale values result in a stable configuration. These gains, and a tight pitch attitude loop closure with pitch integral added, were used at the beginning of free flight in each run after the model had attained speed and was released in roll, yaw, side velocity, and pitch. After a few seconds, when the model was settled in its trimmed equilibrium, the roll and yaw attitude and rate gains were switched to their test values and a well-defined input pulse was applied. The tight loop closures were also used to establish the aileron bias setting which was to assure that the undisturbed model would move along the track, remaining close to the center of its limited lateral travel.

The three loop closures used in the test series were roll attitude and roll rate to differential collective and yaw rate to ailerons. In order to establish the ideal cross-control gain from differential collective to ailerons, the model was locked in roll. Differential collective inputs were applied in a series of runs resulting in various yaw rates depending on the cross-control gain setting. The perfect value, $K_{a\beta} = 0.18$, was found by interpolation. Besides the perfect value, twice this value and zero were used as variations of this parameter. Characteristic lateral runs are shown in Figures 26 through 31.

Run 448 shows the tightness of the control loops with the 1 f.s. gain values and perfect aileron uncoupling. Because of the tight feedback loops the shape of the input pulse is followed by the roll angle with only a very small lag, and no other transient motion occurs. Run 449 differs from the preceding one only in $K_{a\beta} = 0$ instead of 0.18; there is no noticeable difference because the tight yaw rate loop closure makes the control coupling ineffective. This is verified by Run 450, in which the yaw rate feedback was zero. The pronounced effect of the control coupling shows in the ψ response.

Run 467 (Figure 27) was made with 1/4 f.s. feedback gain settings, and for Run 470 the gains were reduced further to 1/8 f.s. Runs 471 and 475 are the same but with $K_{a\beta} = 0$ and $K_{a\beta} = 0.36$ respectively; the effect of the $N_{\delta\beta}$ control coupling is quite marked because of the reduced yaw rate feedback.

Runs 477 and 478 in Figure 28 were made with no roll attitude feedback and with reduced rate feedbacks. $K_{\dot{\psi}}$ was 1/8 f.s. in both cases; $K_{\dot{\phi}}$ was 1/4 f.s. and 1/8 f.s. respectively. There is no marked difference between these two runs except that the reduced tightness of the roll rate loop shows somewhat in Run 478. $K_{a\beta}$ was 0.18 in both of these runs. In an attempt to excite the oscillatory mode, an aileron input was applied in Run 490 in which a large yaw rate gain (1 f.s.) was used with only a relatively small $K_{\dot{\phi}} = 1/4$ f.s. for marginal stability.

The runs described so far were made at the trim speed $U_o = 18.6$ ft/sec. The following runs were made at $U_o = 30$ ft/sec, corresponding to a fixed decelerating condition (Figure 29).

Run 506 was made with tight roll rate feedback only ($K_{\dot{\phi}} = 1$ f.s.). This run again clearly shows that without yaw rate feedback the $N_{\delta\beta}$ control coupling has a very strong effect.

Runs 507 and 508 were made with the same reduced feedback gains of 1/4 f.s. and 1/8 f.s., respectively, as were Runs 467 and 470 at trim speed. There are two noticeable differences. The damping of the dominant roll response is somewhat reduced but seems still quite acceptable, and there is a marked difference in the control coupling, indicating a significant deviation of $N_{\delta\beta}$ from the trim speed value.

Run 511 corresponds to Run 475. Run 516 was made with the same gains as run 478.

In Figure 30, two runs with aileron inputs are shown both with the same gains but Run 485 at trim speed (U_o = 18.6 ft/sec) and Run 518 at the fixed decelerating condition (U_o = 30 ft/sec), with a marked Dutch roll mode being excited at the higher speed.

The last group of runs was made at U_o = 15 ft/sec, corresponding to a fixed accelerating condition. Run 541 (Figure 31) is to be compared with the low gain (1/8 f.s.) Run 478. An increase in damping is indicated by the much smoother responses. The improvement was sufficient to produce a long run without hitting any stops.

Run 542 corresponds to Run 477 with no marked difference showing. Similarly, Runs 543, 544, 545, and 546 are hardly distinguishable from the corresponding trim velocity Runs 475, 471, 470, and 467 except for an indication of a somewhat more stable spiral mode.

The comparisons of the fixed accelerating and decelerating conditions indicate the apparent destablizing effect of deceleration more than a stabilizing effect of acceleration. The most marked difference is in the cross-control coupling $N_{\delta\beta}$ between trim speed and the deceleration condition. Deviations due to acceleration-deceleration can be diminished if large constant feedback gains are used. Adequate stability could be achieved with smaller gains if these were programmed to compensate for deceleration as well as airspeed effects.

CONCLUSIONS

1. The transition region of VTOL aircraft can generally be characterized by a lack of a short-period longitudinal mode. Such a mode can be created by applying attitude and attitude rate feedback. A short-period pole pair which remains in the vicinity of its desired location can be produced using constant gains throughout the hover and transition region.

2. The feedback gains can be determined using an approximate stability derivative model for the transition region. Accurate knowledge of the often complicated behavior of stability and control derivatives in this region is not necessary for a satisfactory longitudinal and lateral feedback design.

3. The problem of control cross-coupling from roll to yaw can be practically eliminated by using a high gain yaw rate feedback loop, so that artificial control cross-coupling may be unnecessary.

4. Free-flying model experiments showed that tight loop closures must be used in decelerating transition in order to make the closed-loop dynamics relatively independent of the amount of deceleration used.

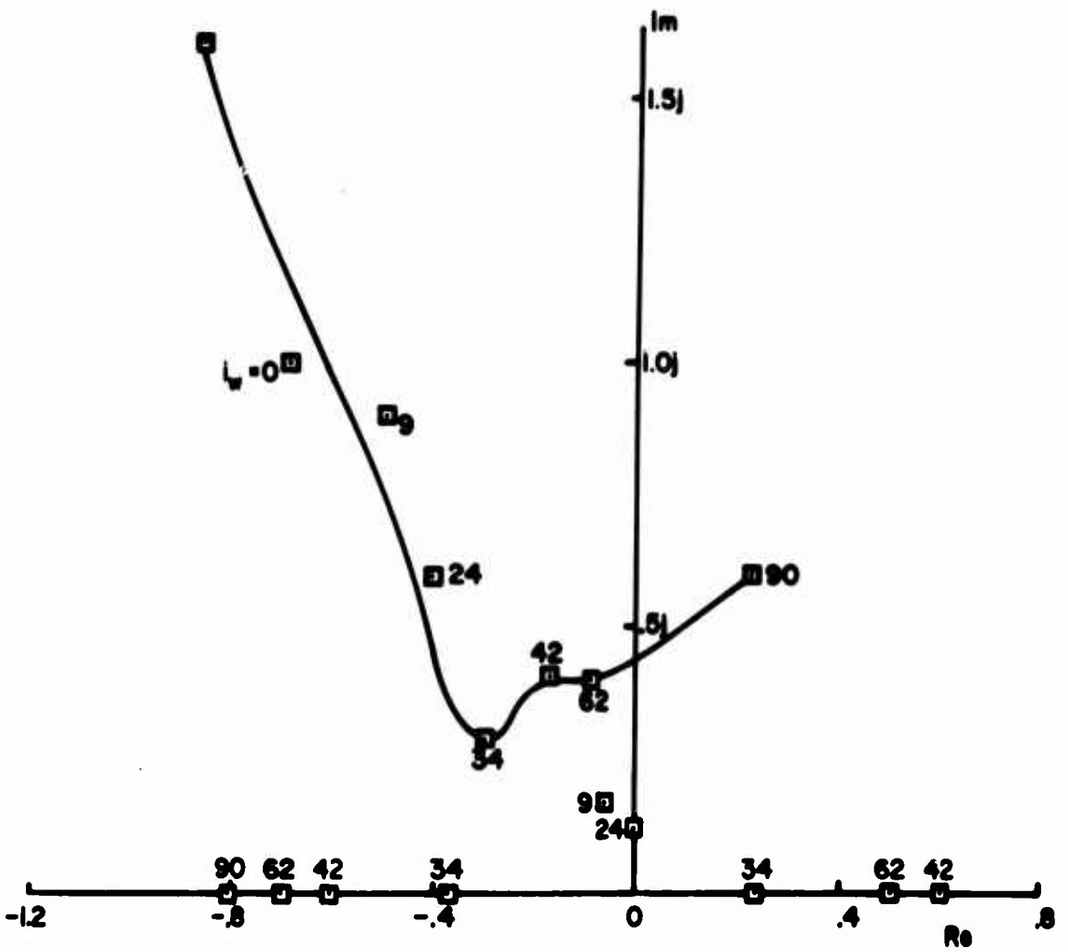

Figure 1. Characteristic Roots of the Tilt-Wing VHR-447 Tri-Service VTOL Aircraft.

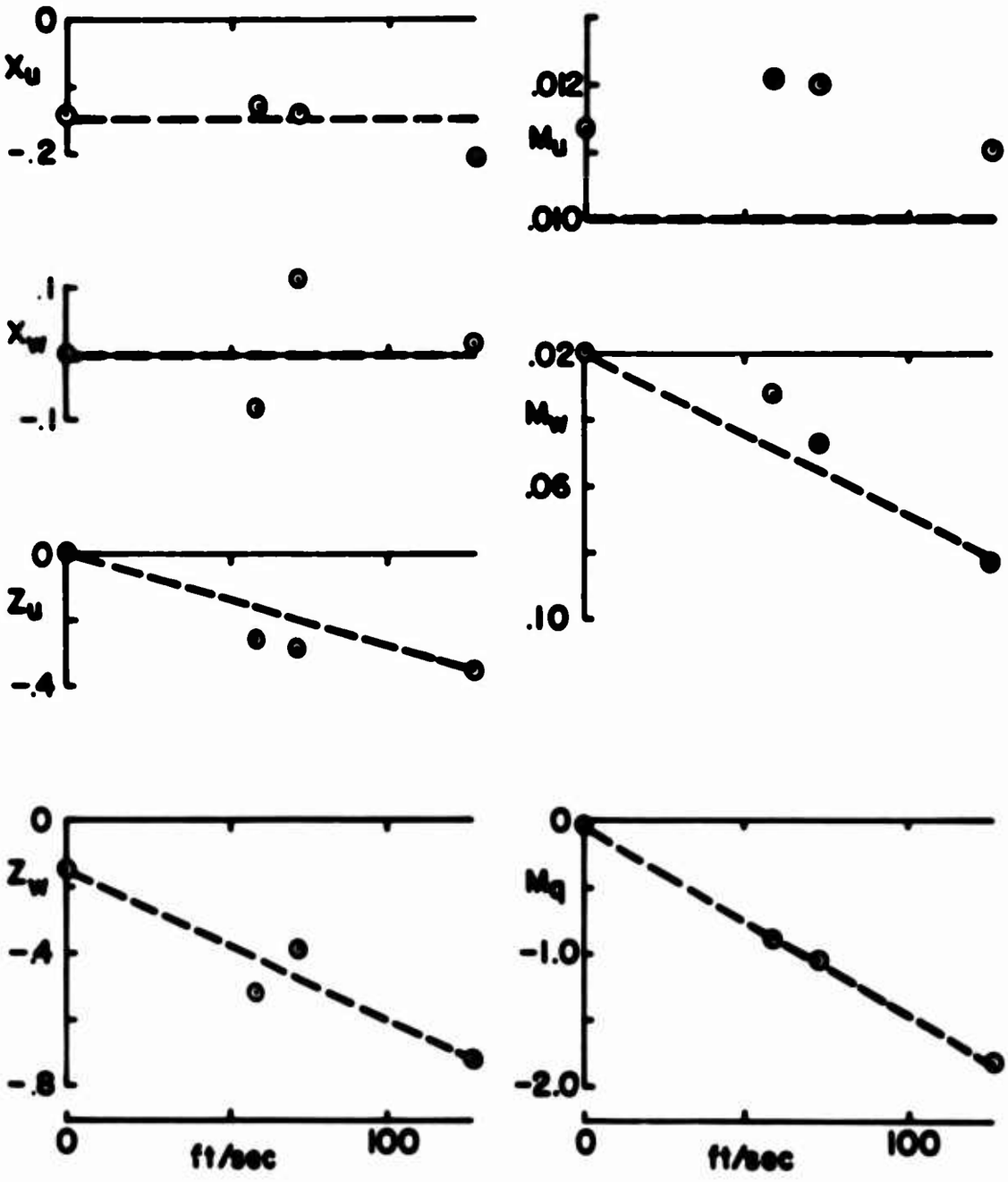

Figure 2. VZ-4 Longitudinal Stability Derivatives and Their Approximations.

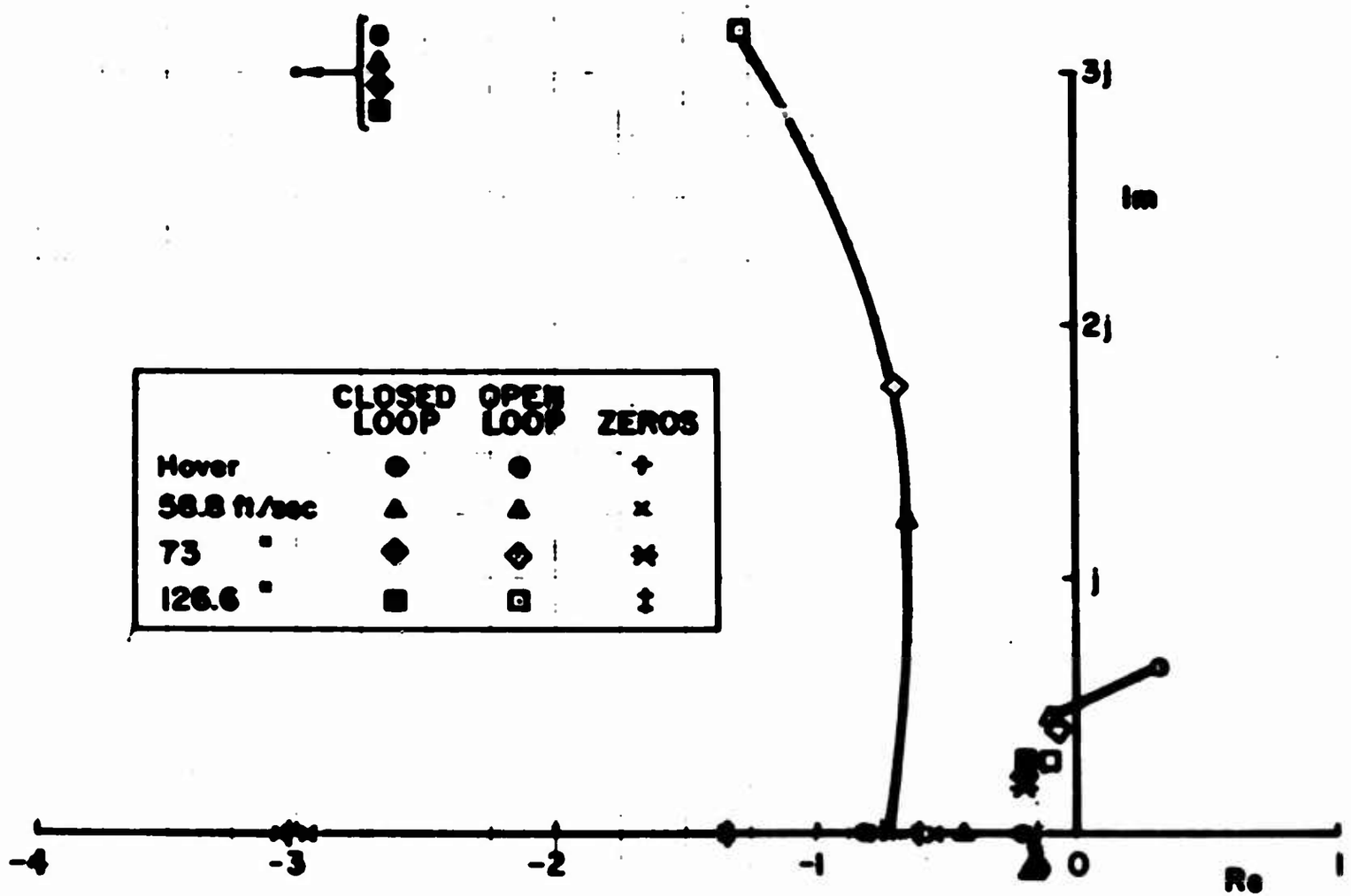

Figure 3. Transfer Function Poles and Zeros for VZ-4 With Pitch Attitude and Rate Feedbacks for Predetermined Short-Period Mode, Using Known Derivatives.

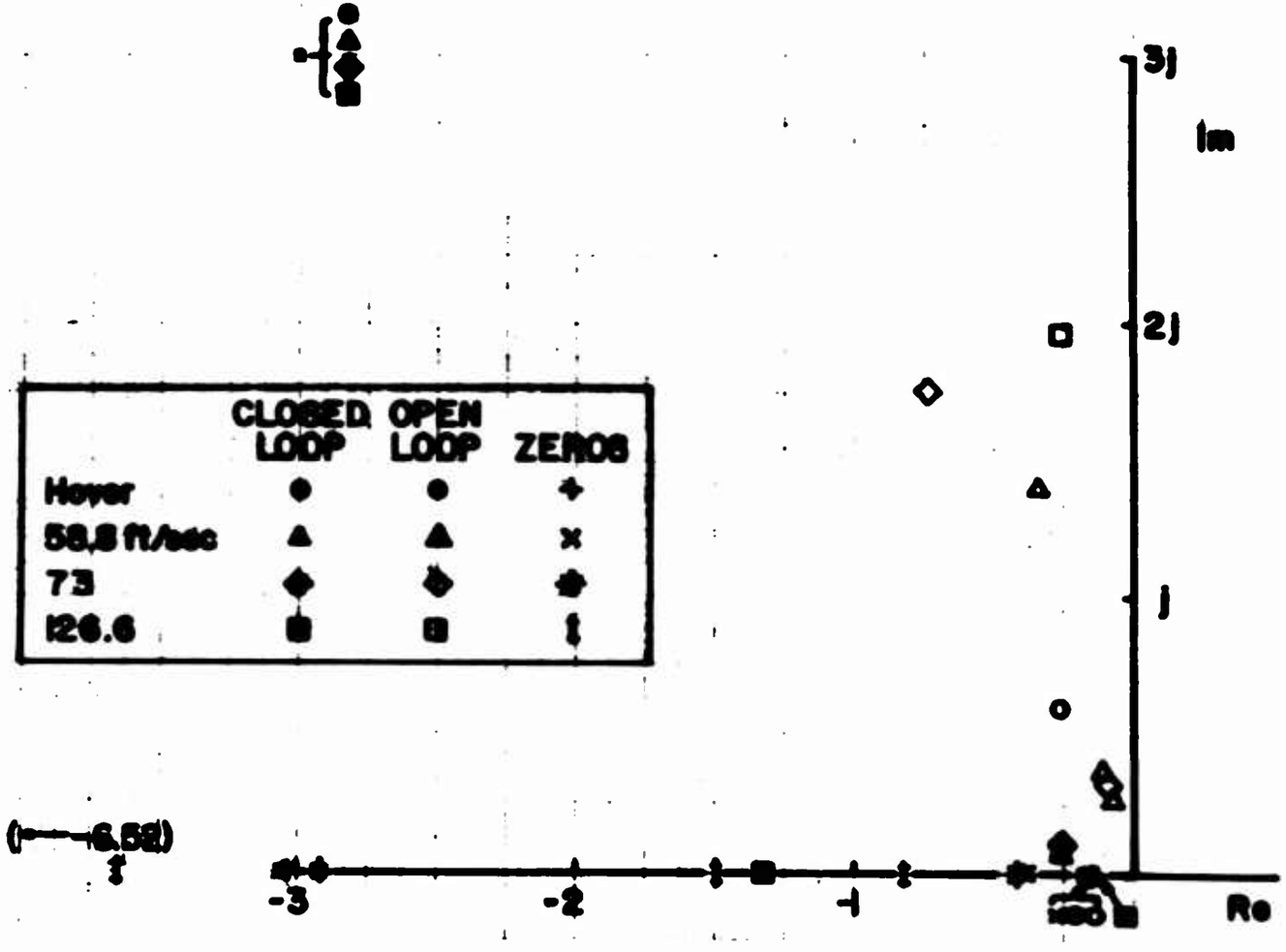

Figure 4. Transfer Function Poles and Zeros for VZ-4 With Pitch Attitude and Rate Feedbacks for Predetermined Short-Period Mode, Using Approximations for the Derivatives.

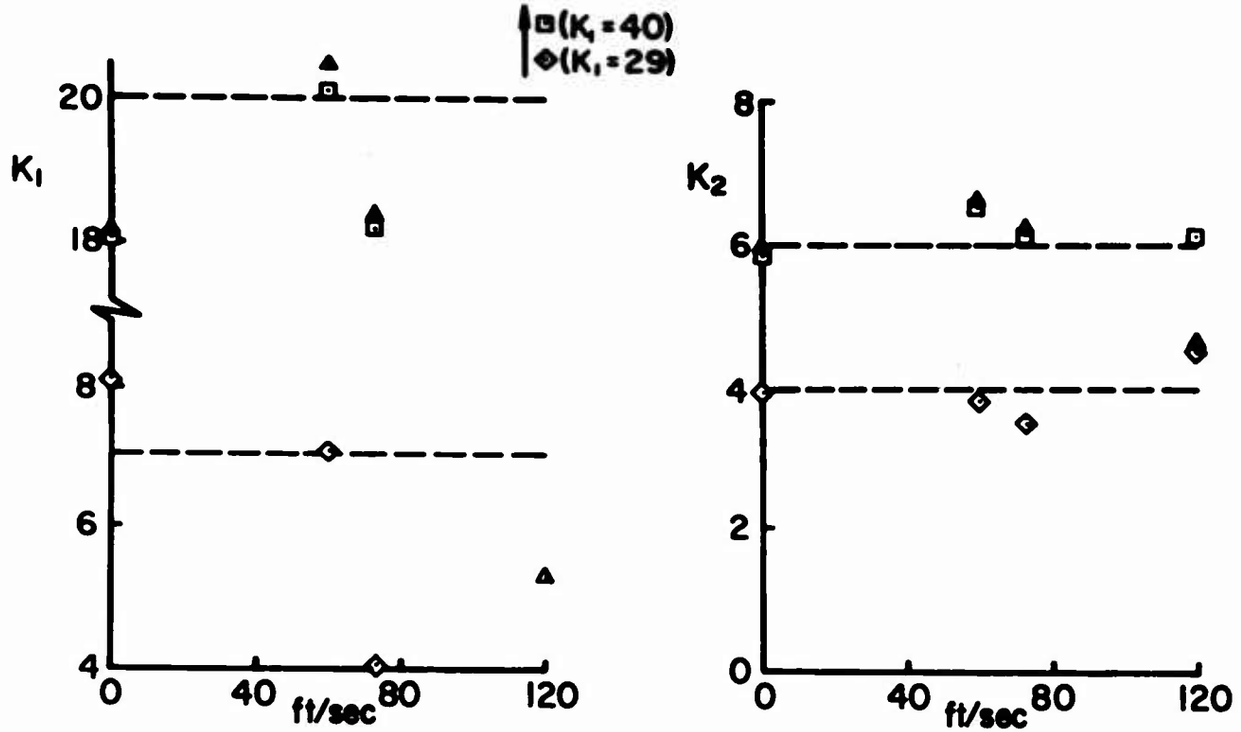

Figure 5. Feedback Gains for Predetermined Short-Period Closed-Loop Modes of VZ-4 at -3 ± 3j and -2 ± 2j.

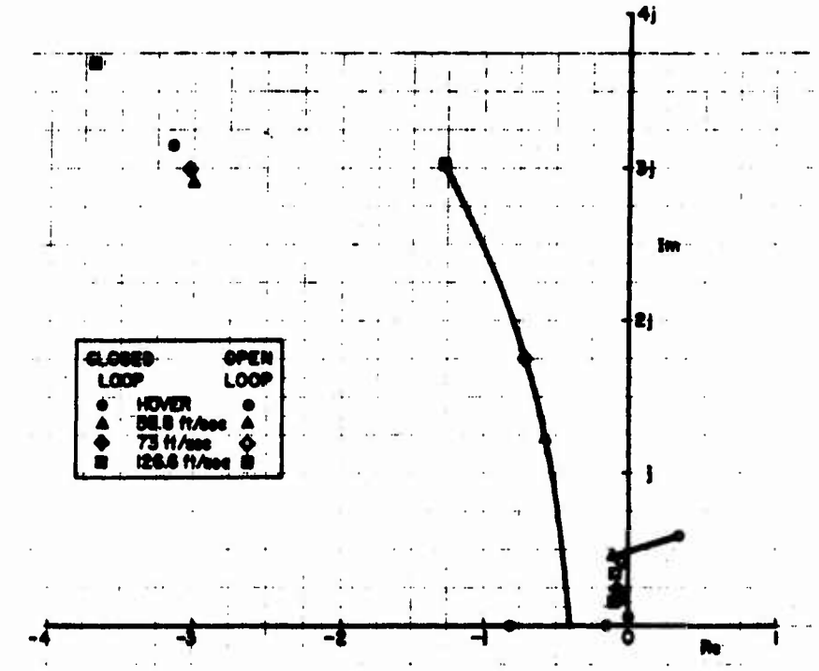

(a)

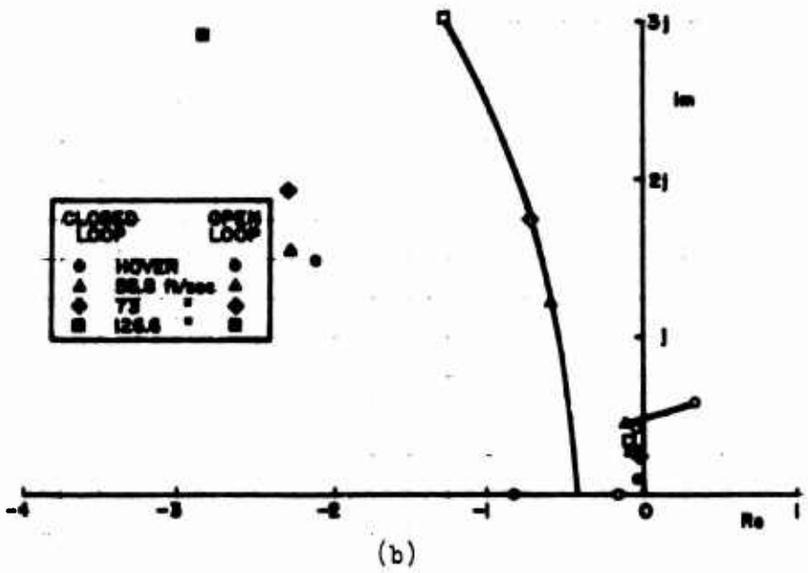

(b)

Figure 6. Transfer Function Poles for VZ-4 With Fixed Pitch Attitude and Rate Feedbacks for Short-Period Modes near $-3 \pm 3j$ and $-2 \pm 2j$.

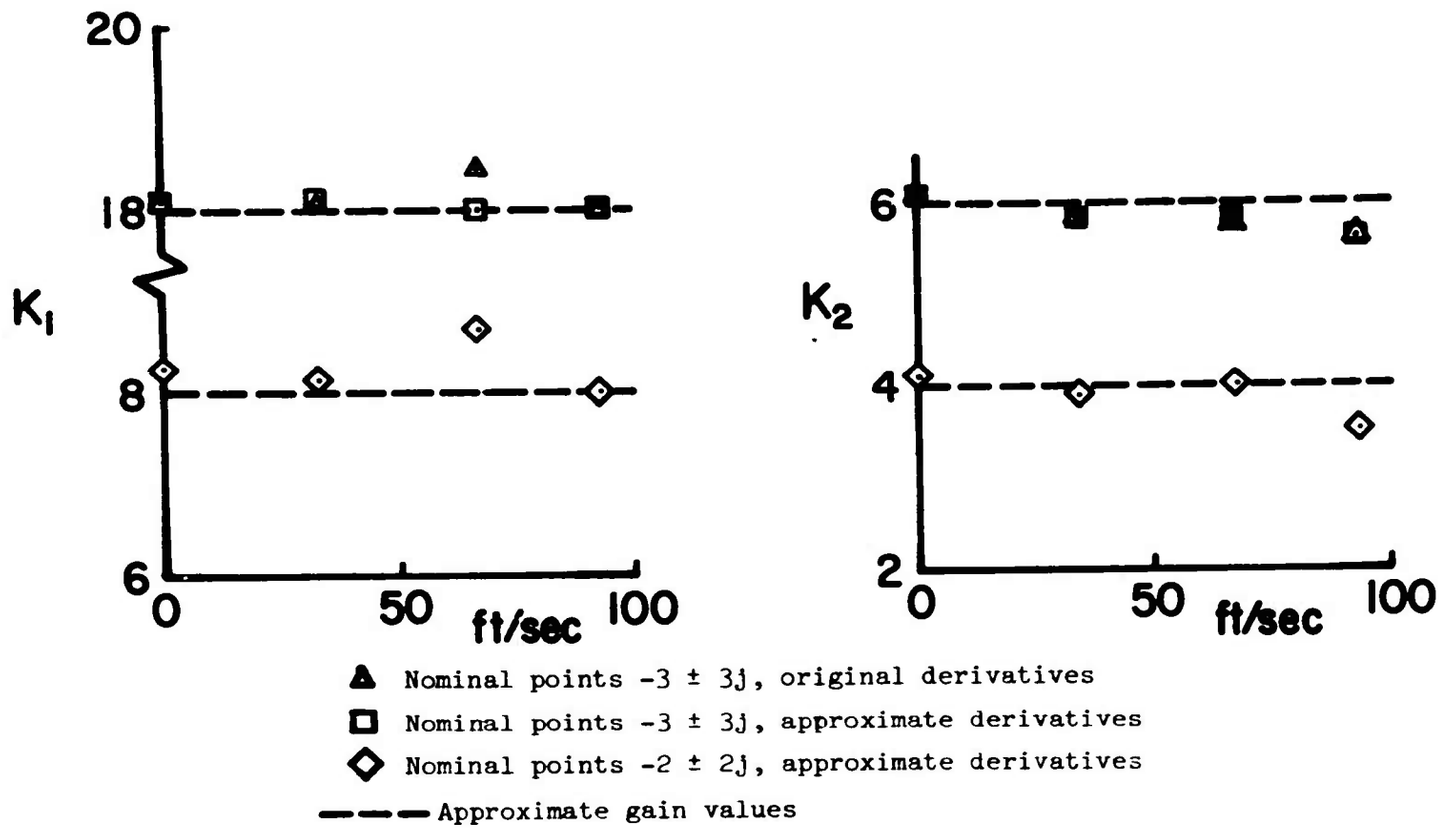

Figure 7. Feedback Gains for Predetermined Short-Period Closed-Loop Modes of the XC-142 at -3 ± 3j and -2 ± 2j.

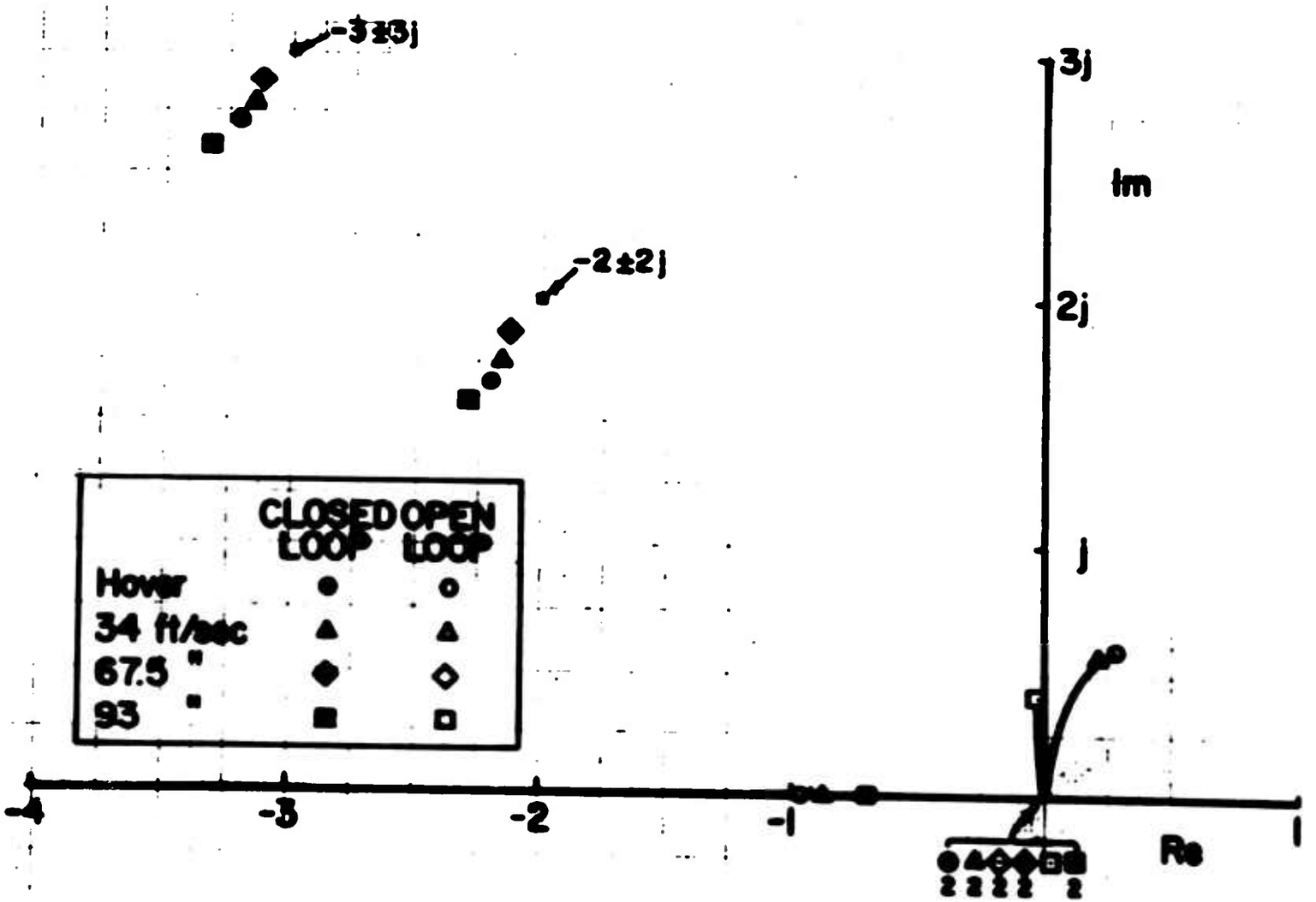

Figure 8. Transfer Function Poles for a Simplified Model of the XC-142 With Fixed Pitch Attitude and Rate Feedbacks, for Closed-Loop Short-Period Modes Near -3 ± 3j and -2 ± 2j.

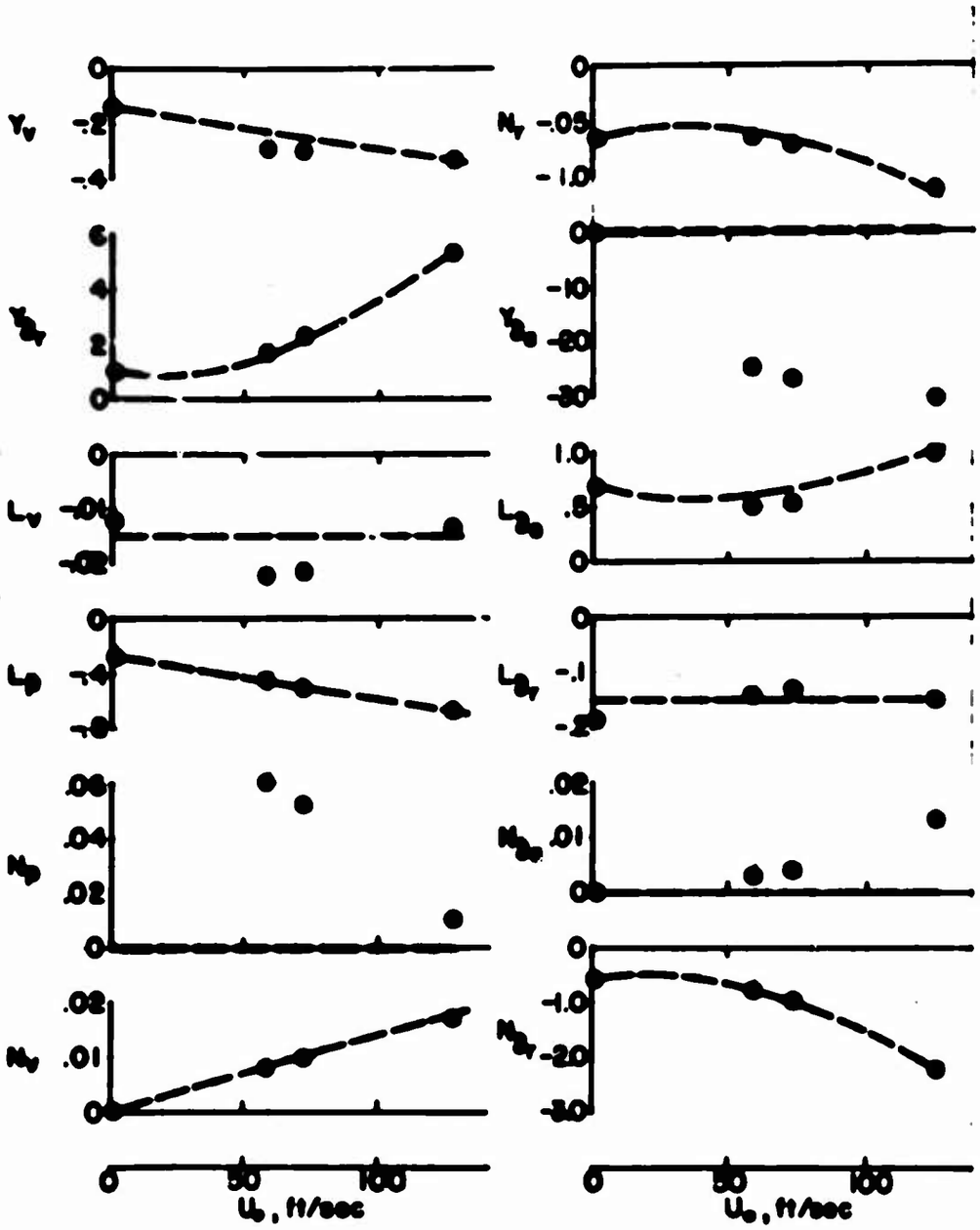

Figure 9. VZ-4 Lateral-Directional Stability Derivatives and Their Approximations.

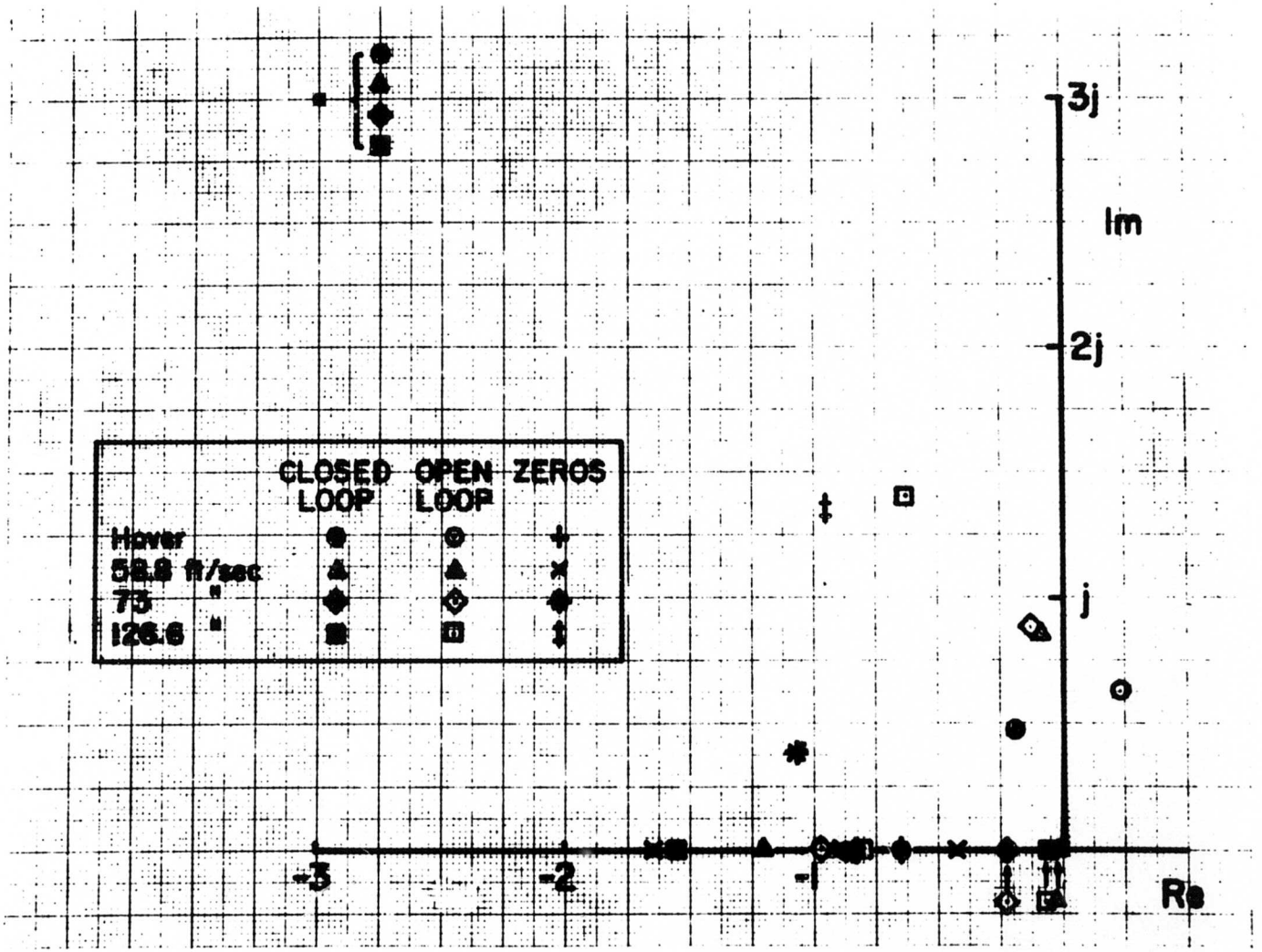

Figure 10. Roll Angle to Roll Control Transfer Function Poles and Zeros of VZ-4 With Feedback Applied for Predetermined Dominant Rolling Mode.

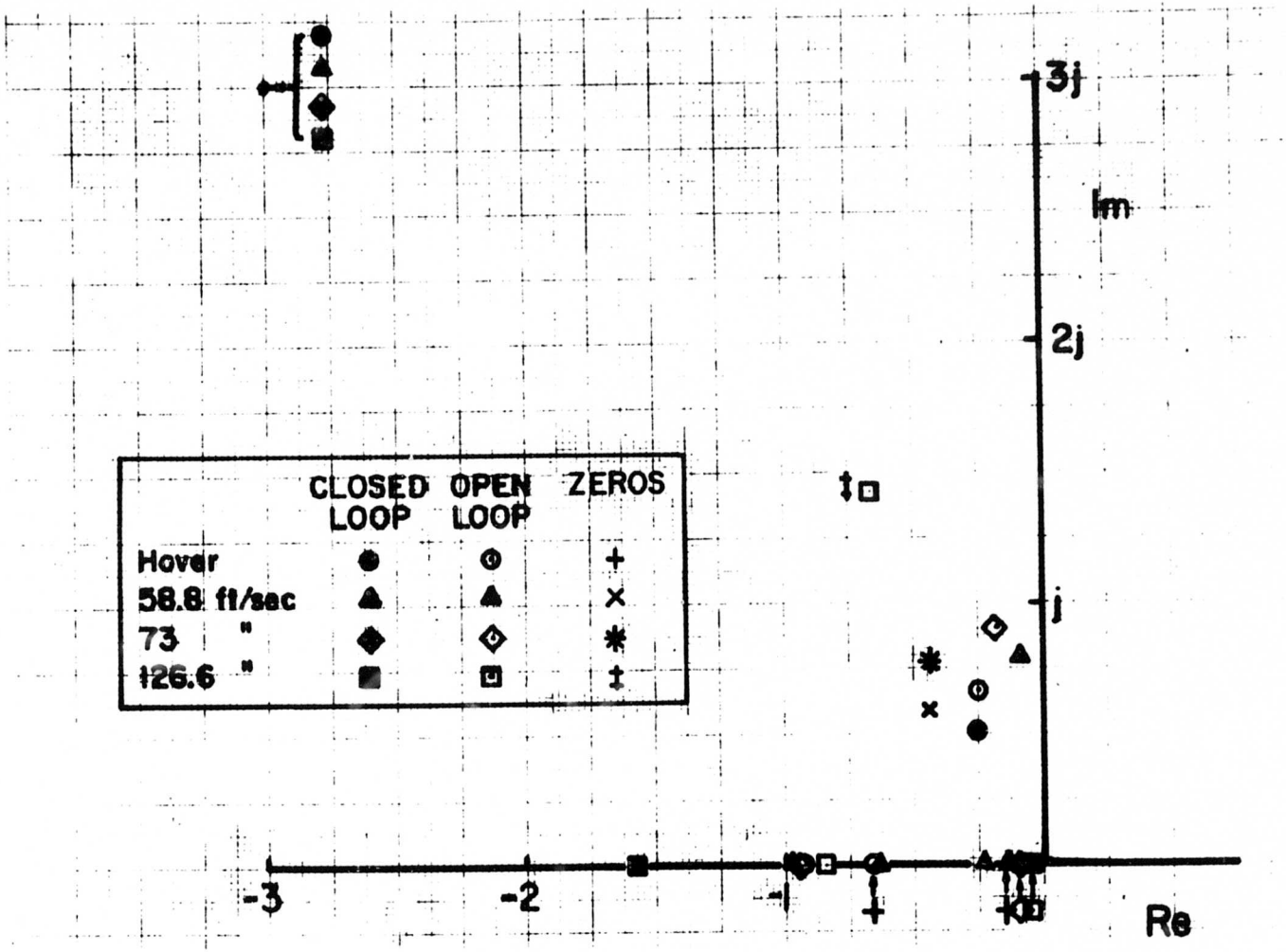

Figure 11. Roll Angle to Roll Control Transfer Function of VZ-4 Approximate Model With Feedback Applied for Predetermined Dominant Rolling Mode.

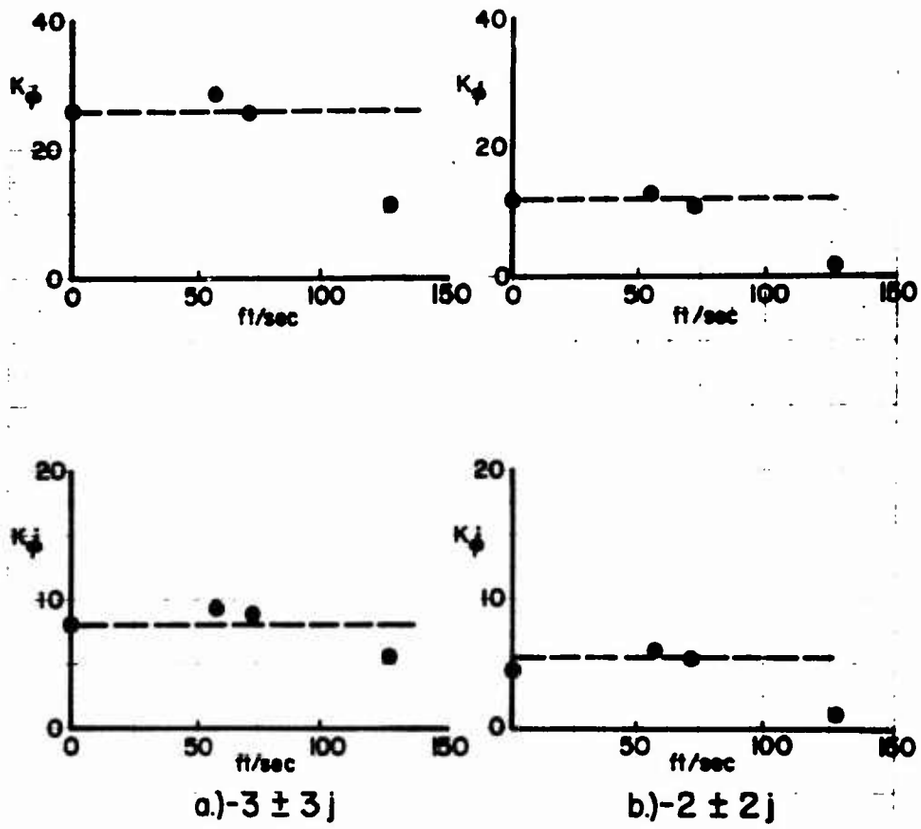

Figure 12. Roll Angle and Roll Rate Feedback Gains for VZ-4 Approximate Model, Calculated for Predetermined Dominant Rolling Mode.

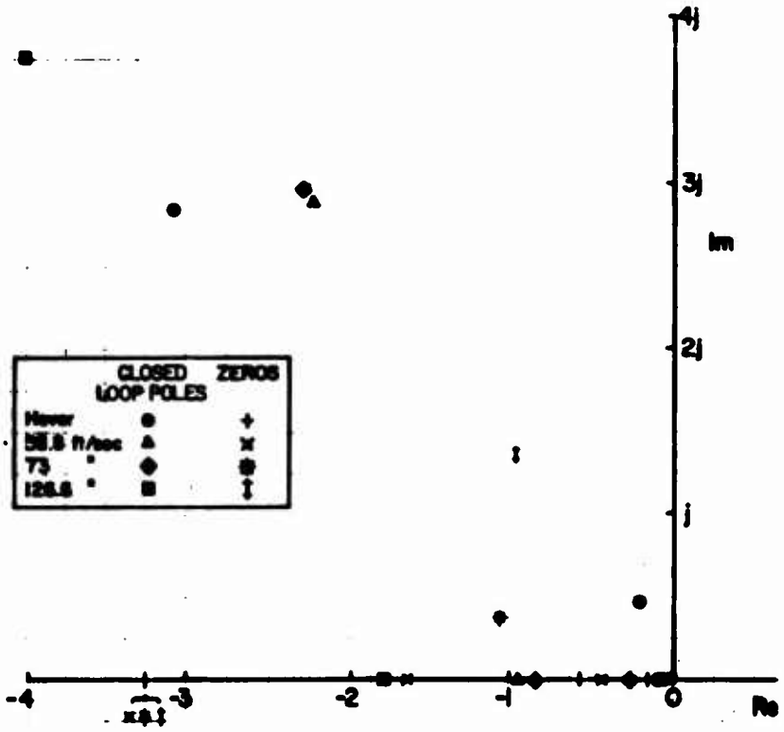

(a)

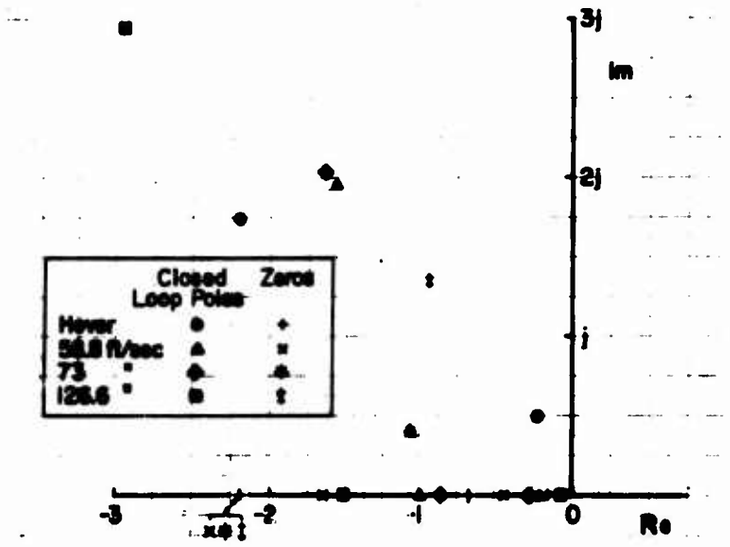

(b)

Figure 13. Closed-Loop Transfer Function Poles and Zeros for the VZ-4 With Roll Angle and Roll Rate Feedback Gains Determined Using an Approximate Model, for the Dominant Rolling Mode to be Near $-3 \pm 3j$ and $-2 \pm 2j$.

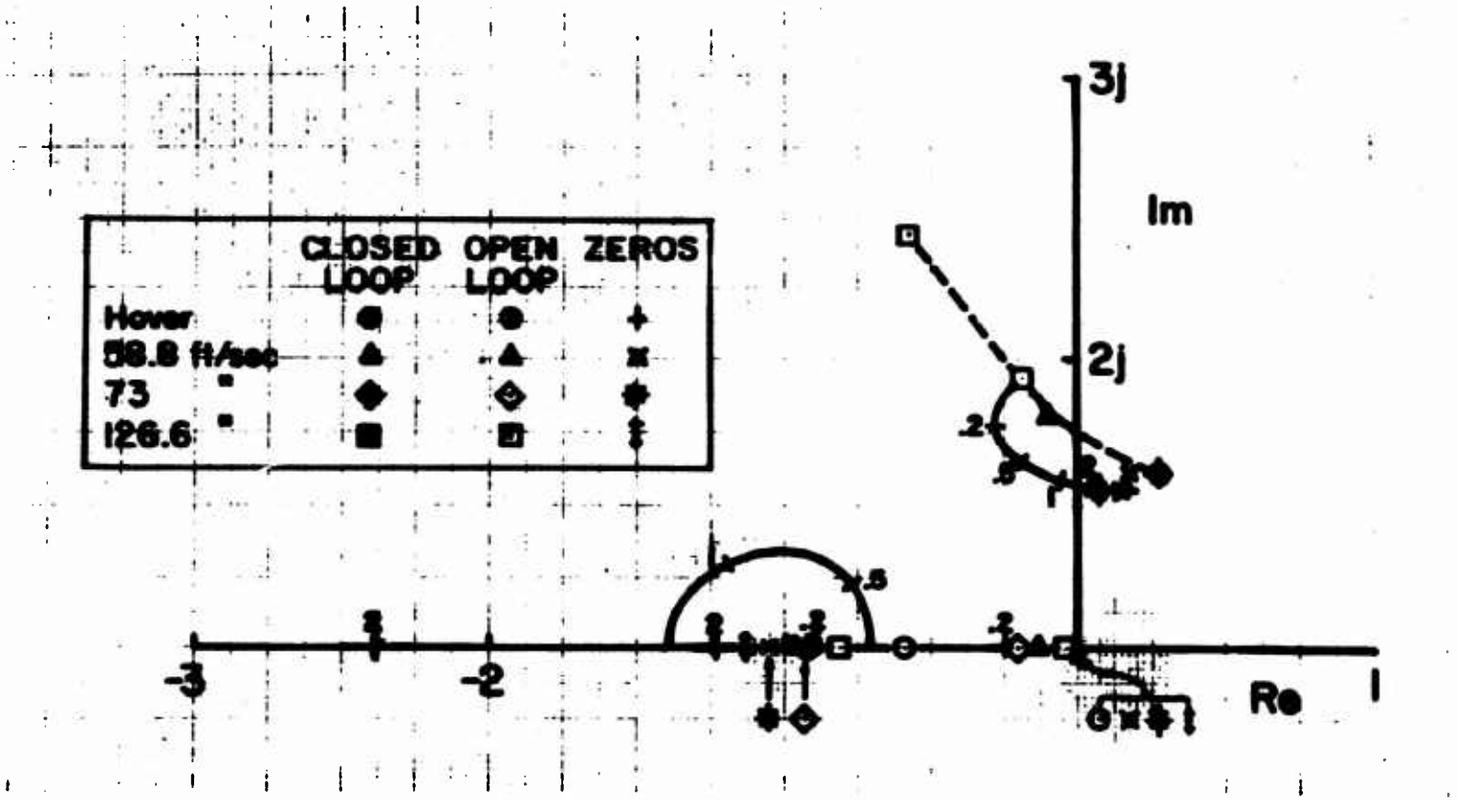

Figure 14. Yaw Rate to Rudder Transfer Function Poles and Zeros for VZ-4 With Constant Cross-Control Gain From Rudder to Roll, K_{ar} = .2.

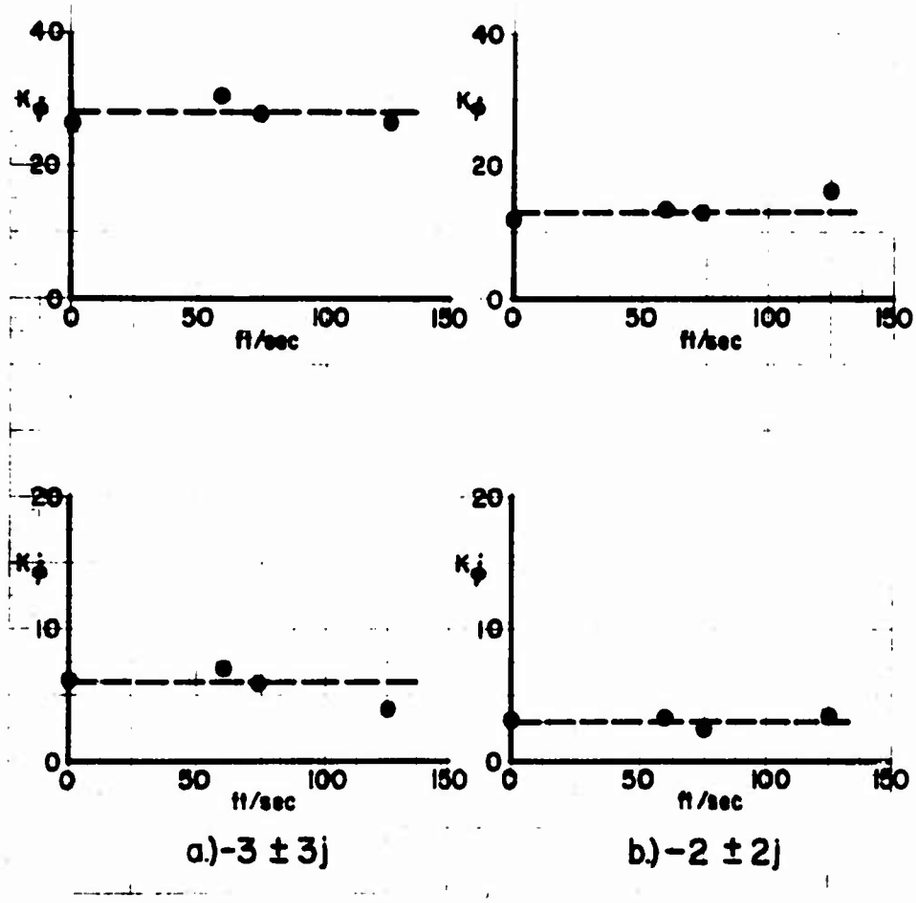

Figure 15. Roll Angle and Roll Rate Feedback Gains for VZ-4 With Tight Yaw Rate Loop Closure, Calculated for Predetermined Dominant Rolling Mode.

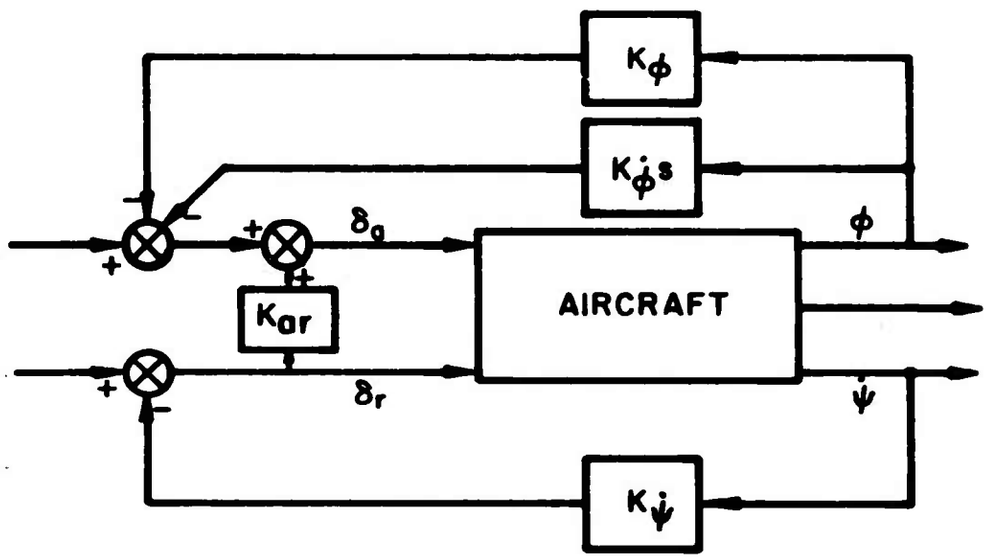

Figure 16. Block Diagram of Lateral-Directional Feedback Loops and Cross-Control.

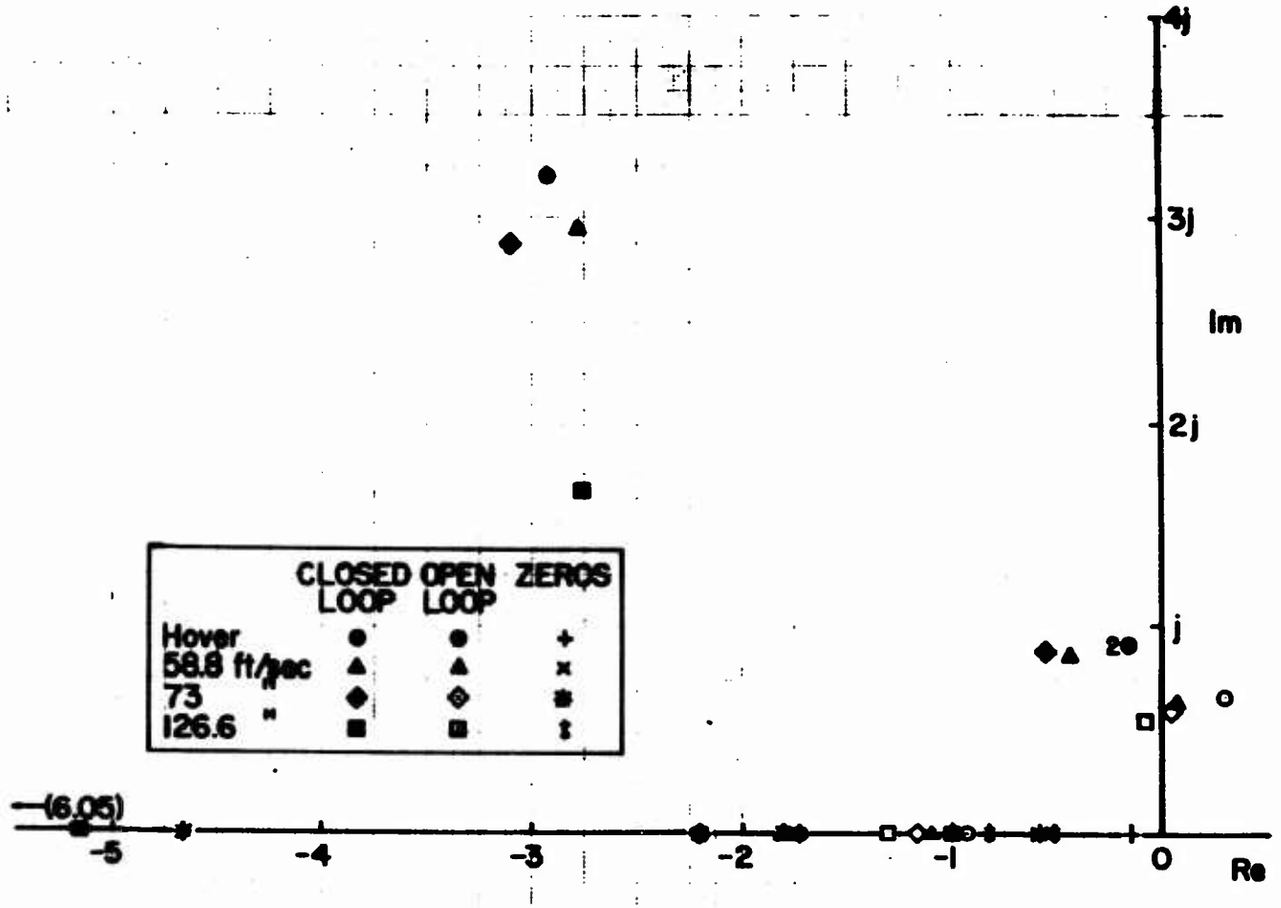

Figure 17. Roll Response Transfer Function Poles and Zeros of VZ-4 With Constant Cross-Control K_{ar} = .2 and Constant Yaw Rate Feedback Gain $K_{\dot{\psi}}$ = 2 Throughout Transition.

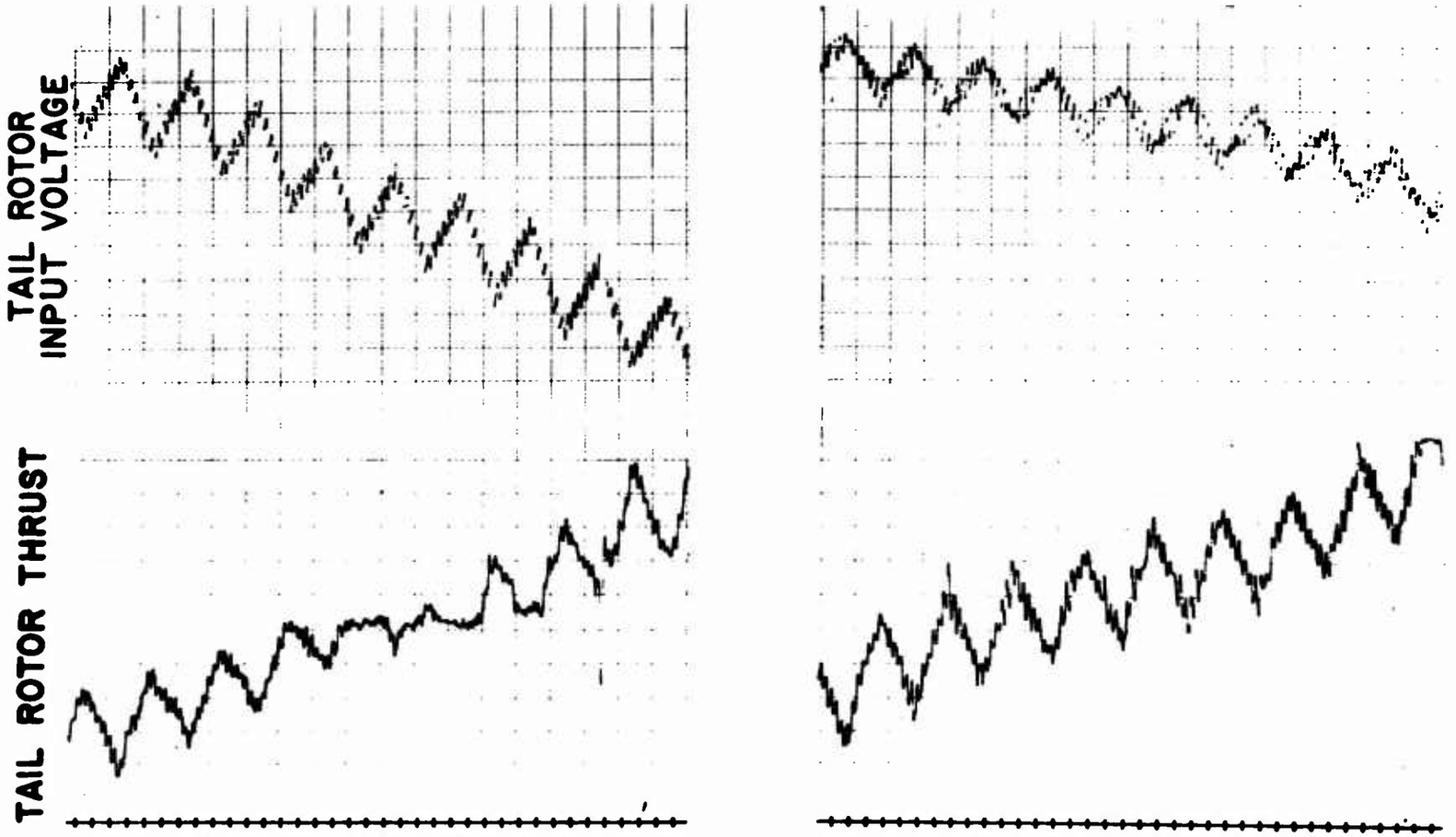

Figure 18. Illustration of Tail Rotor Thrust Vs. Collective Characteristic of XC-142 Model.

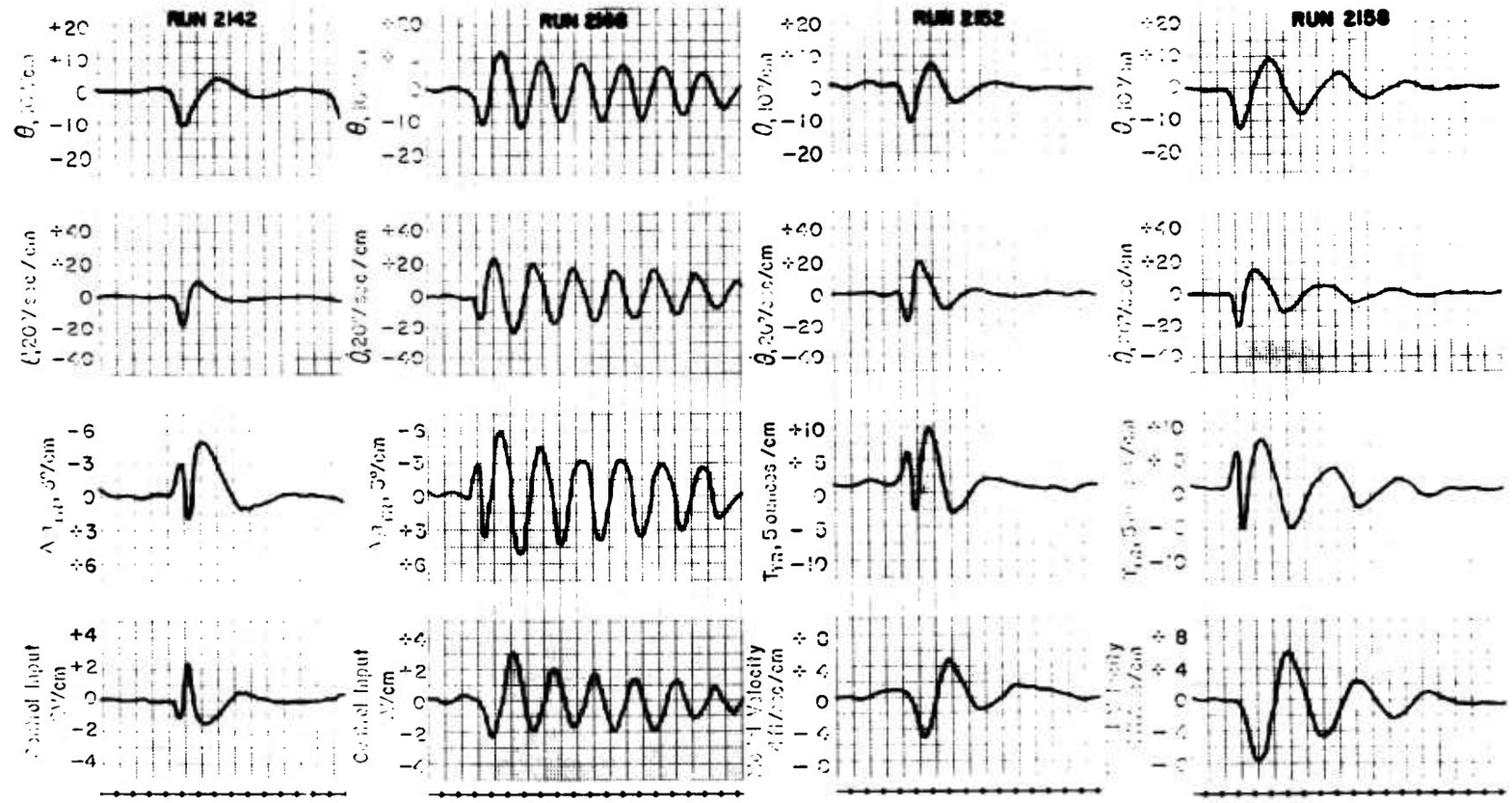

Figure 19. Longitudinal Two-Degrees-of-Freedom Runs With XC-142 Model in Hover.

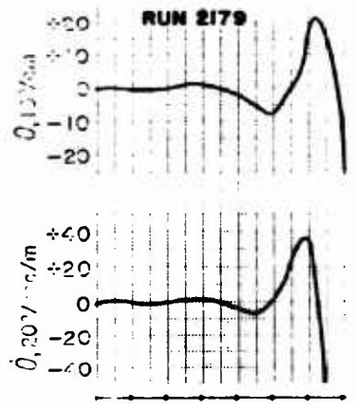

Open Loop

Run 2179

Figure 20. Longitudinal Open-Loop Response of XC-142 Model in Hover.

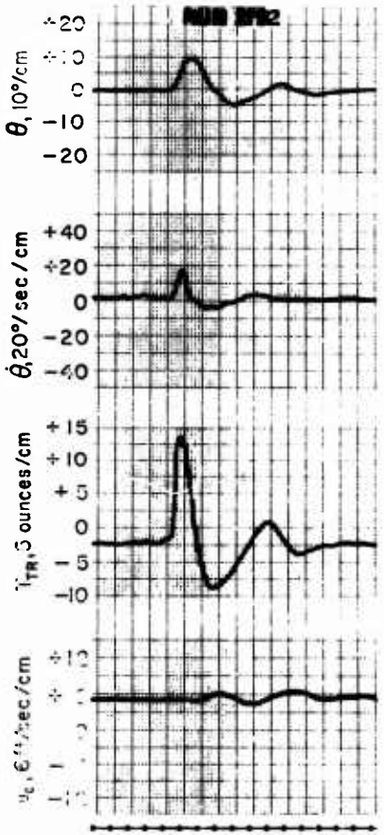

3DF $K_\theta = 1$, $K_{\dot{\theta}} = 5$

Run 2192

Figure 21. Longitudinal Three-Degrees-of-Freedom Run of XC-142 Model at U_o = 5 ft/sec.

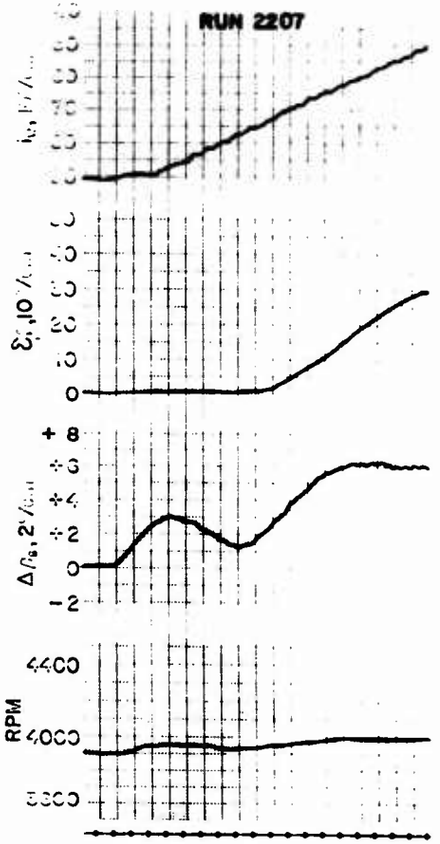

2DF (u, w)

Run 2207

Figure 22. Transition of XC-142 Model Locked in Pitch.

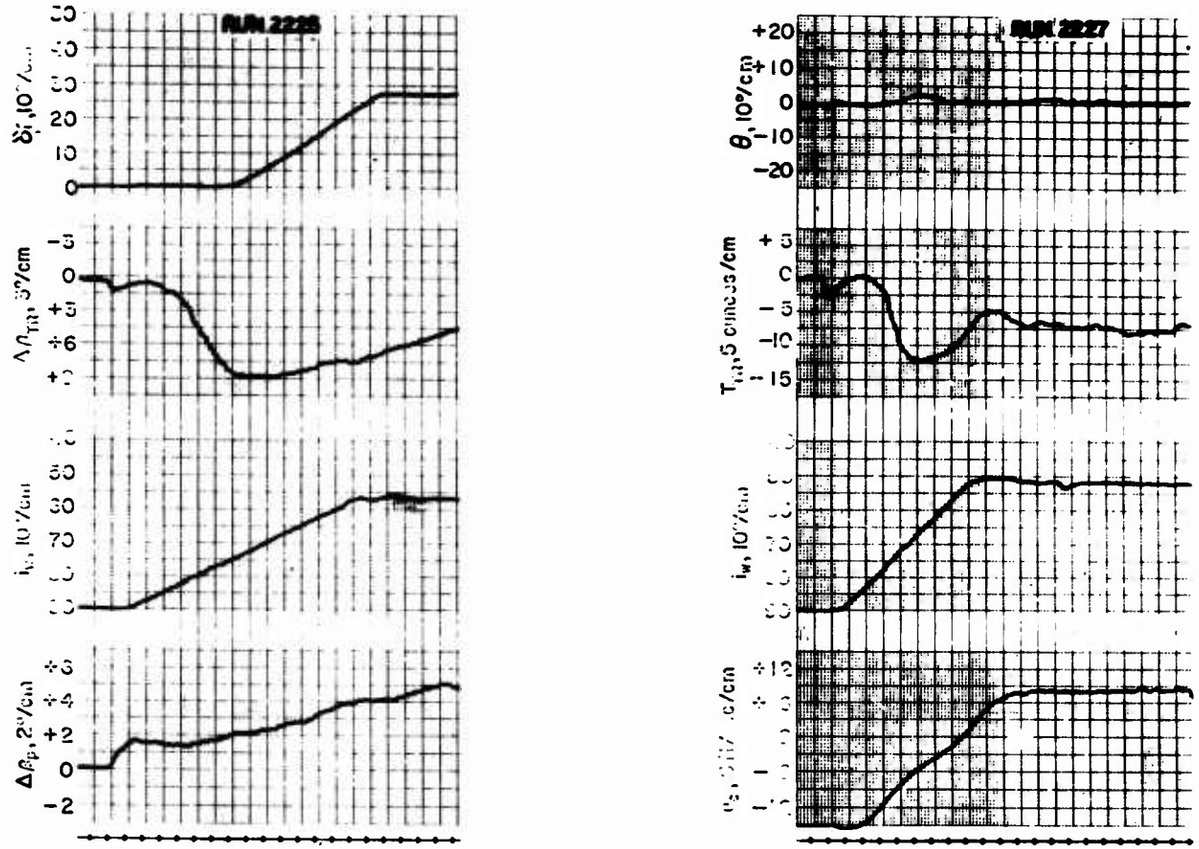

Transition (16 sec)
Run 2225

Transition (8 sec)
Run 2227

Figure 23. Transitions of XC-142 Model, Longitudinal Degrees of Freedom.

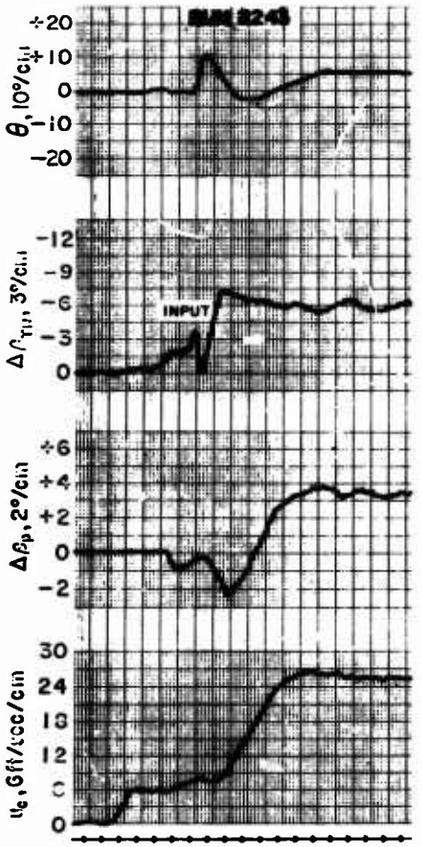

Transition

Run 2243

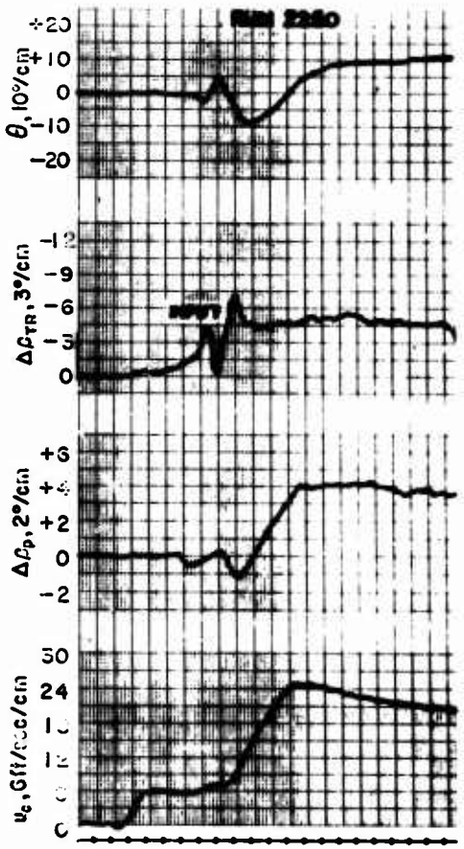

Transition
$K_\theta = .5$, $K_{\dot{\theta}} = 2.5$
Run 2250

Figure 23. Continued.

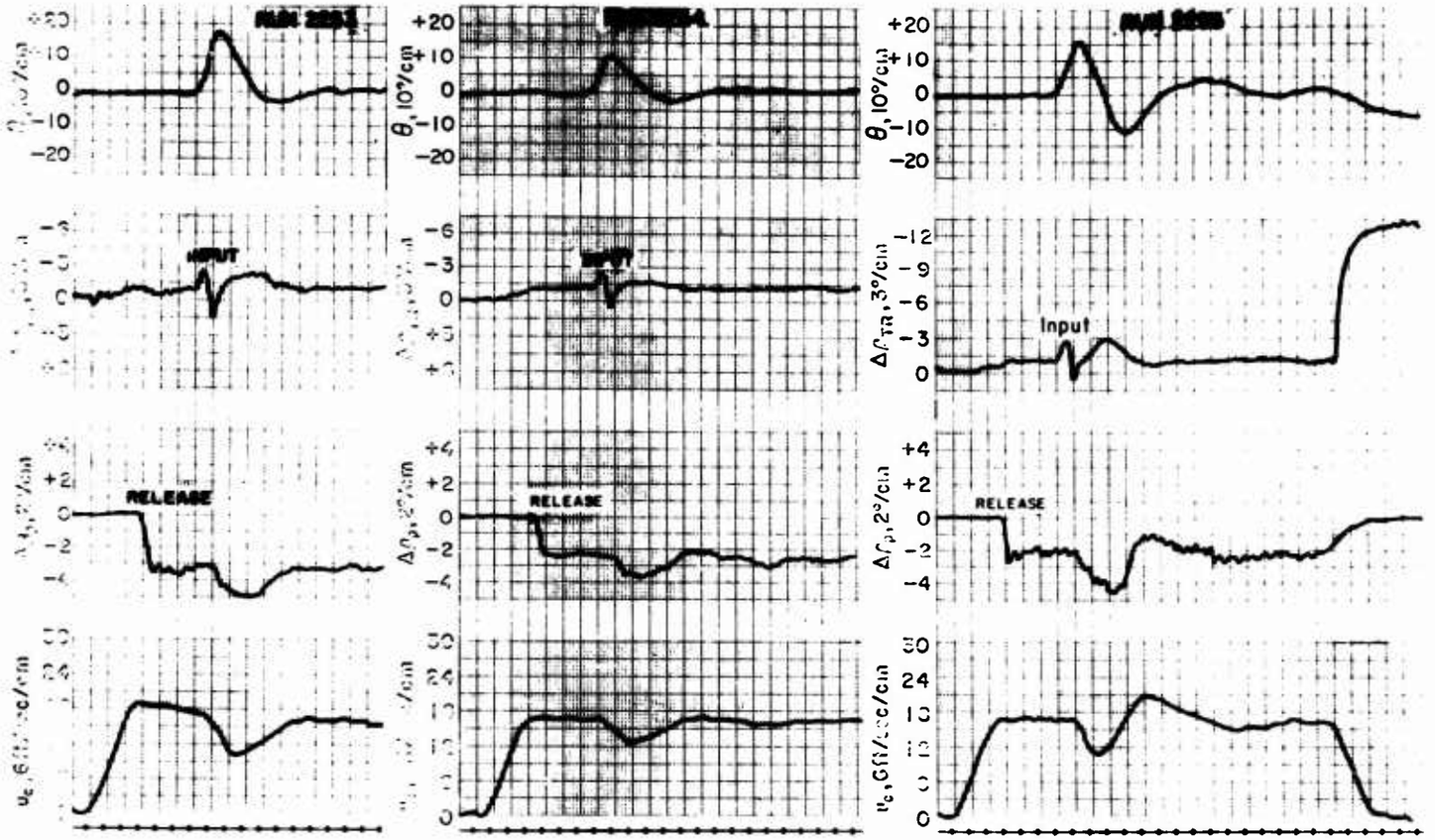

K_θ = .7, $K_{\dot{\theta}}$ = 3.5
Run 2253

K_θ = .35, $K_{\dot{\theta}}$ = 1.75
Run 2254

K_θ = .2, $K_{\dot{\theta}}$ = 1
Run 2225

Figure 24. Dynamic Longitudinal Responses of XC-142 Model at Fixed Point in Transition, $i_w = 60°$, U_o = 18 ft/sec, Simulating an Accelerating Condition.

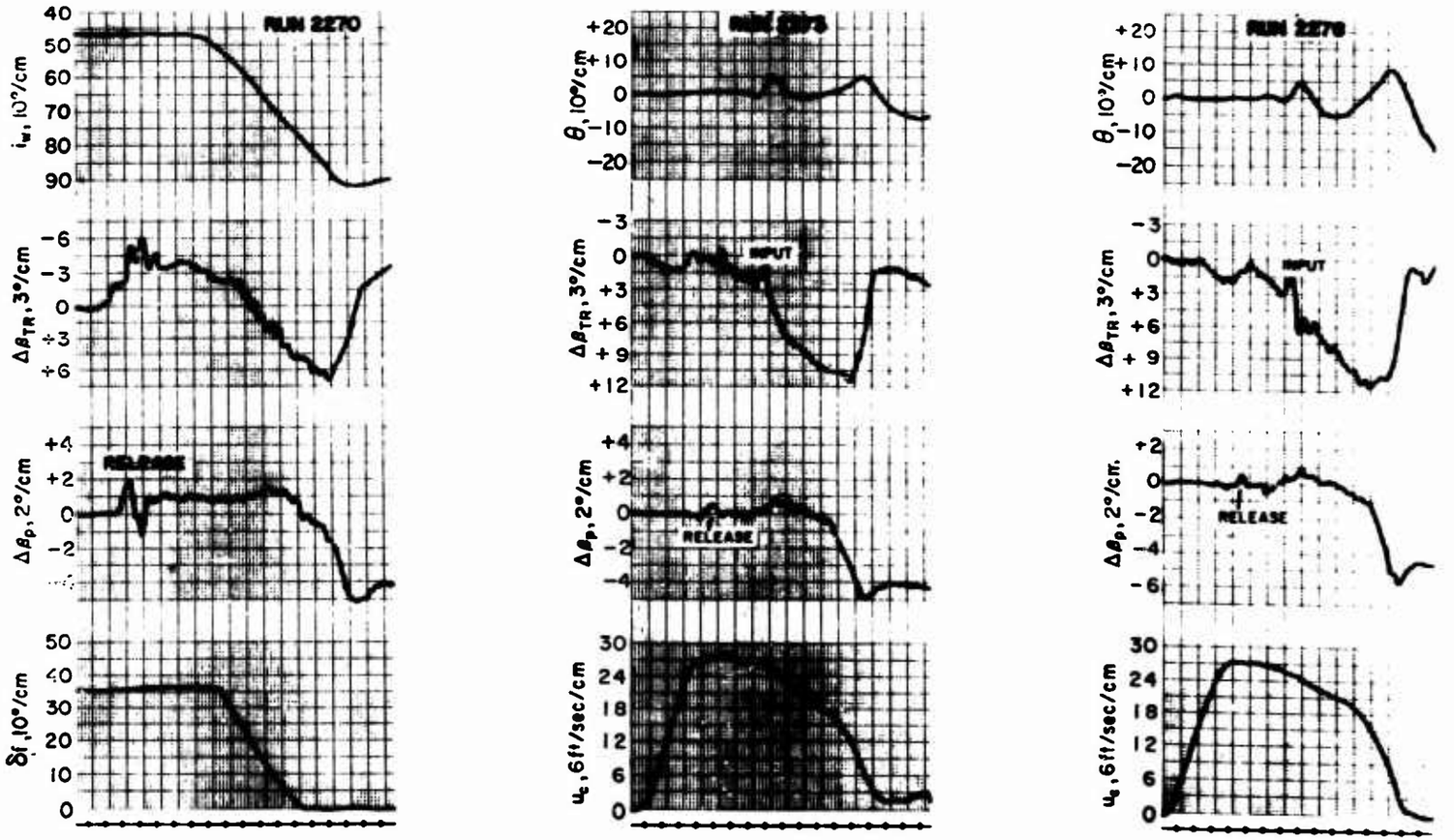

Tight Loops
Run 2270

$K_\theta = .7$, $K_{\dot{\theta}} = 3.5$
Run 2273

$K_\theta = .35$, $K_{\dot{\theta}} = 1.75$
Run 2276

Figure 25. Longitudinal Tests of XC-142 Model in Decelerating Transition.

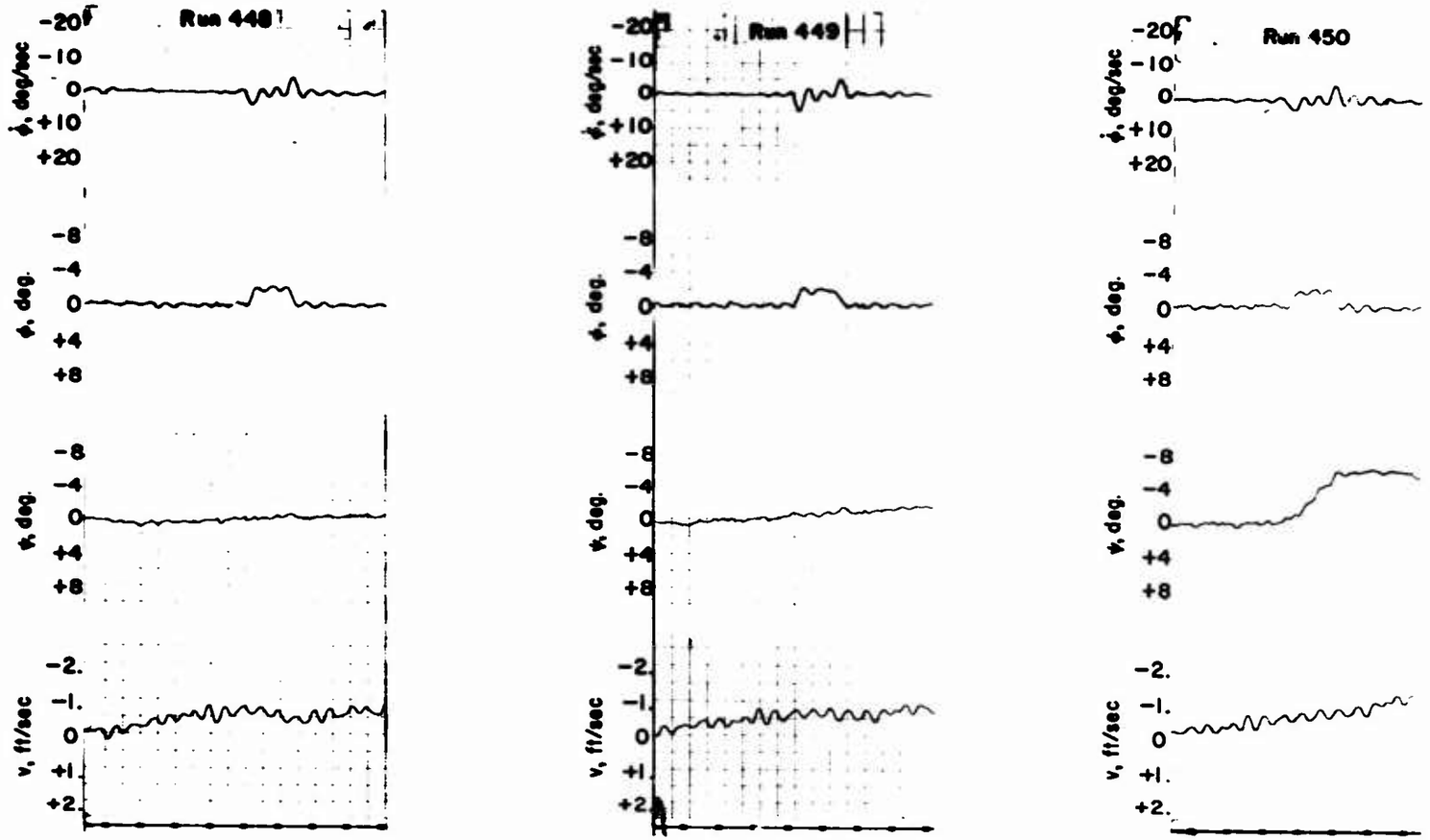

$K_{a\beta}$ = 0.18

Run 448

$K_{a\beta}$ = 0

Run 449

$K_{a\beta}$ = 0. $K_{\dot{\psi}}$ = 0

Run 450

Figure 26. Lateral-Directional XC-142 Model Responses With Feedback Gains Corresponding to 1 f.s. Values ($i_w = 40^o$, $\delta_f = 60^o$, U_o = 18.6 ft/sec).

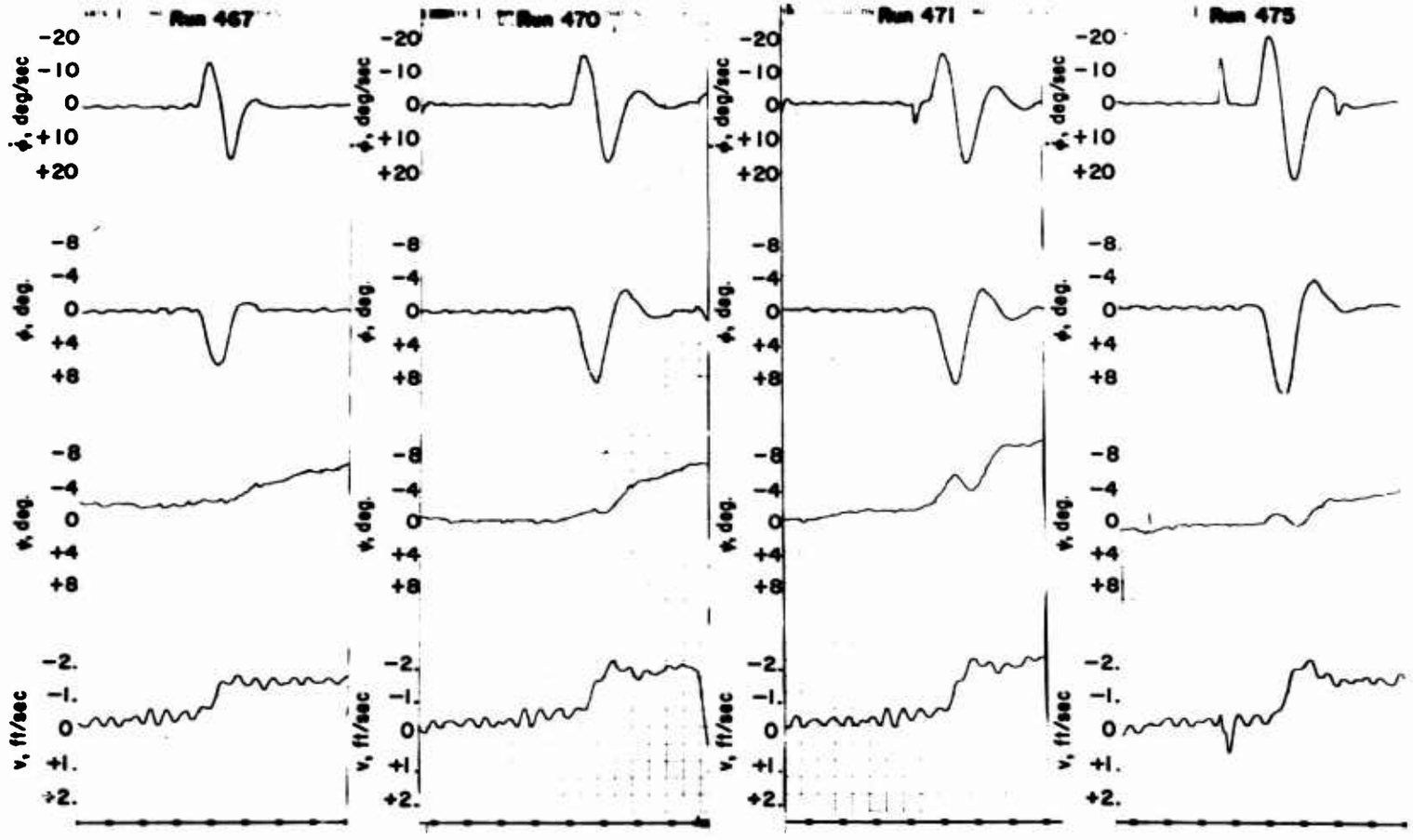

Gains 1/4 f.s. $K_{a\beta}$=0.18 Run 467 | Gains 1/8 f.s. $K_{a\beta}$=0.18 Run 470 | Gains 1/8 f.s. $K_{a\beta}$= 0 Run 471 | Gains 1/8 f.s. $K_{a\beta}$=0.36 Run 475

Figure 27. Lateral-Directional XC-142 Model Responses With Reduced Feedback Gains ($i_w = 40^o$, $\delta_f = 60^o$, U_o = 18.6 ft/sec).

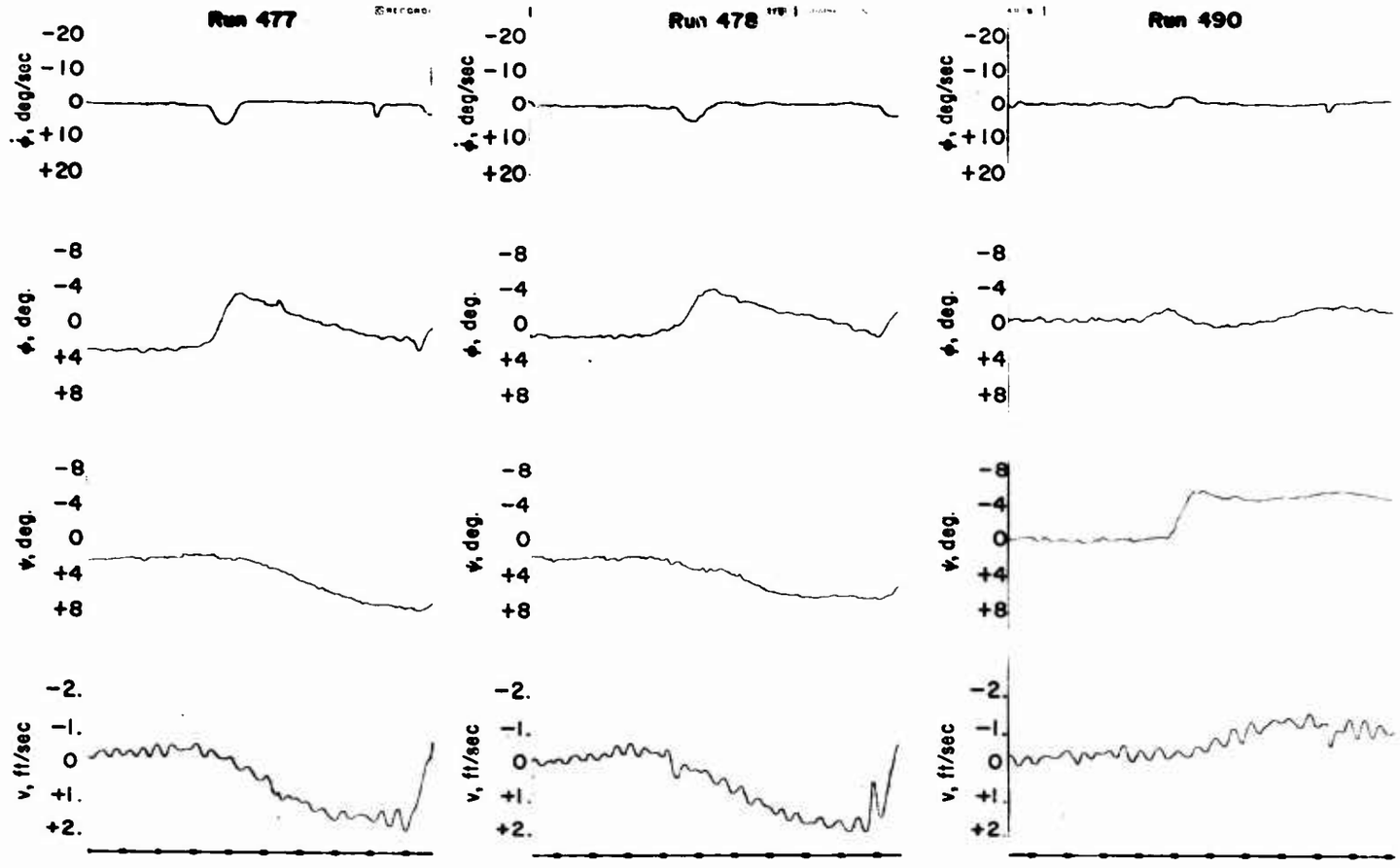

$K_{\dot{\psi}}$ = 1/8 f.s., $K_{\dot{\phi}}$ = 1/4 f.s. Run 477

$K_{\dot{\psi}}$ = 1/8 f.s., $K_{\dot{\phi}}$ = 1/8 f.s. Run 478

$K_{\dot{\psi}}$ = 1 f.s., $K_{\dot{\phi}}$ = 1/4 f.s. Run 490

Figure 28. Lateral-Directional XC-142 Model Responses With Rate Feedbacks Only, With Ideal Cross-Control Gain $K_{a\beta}$ = 0.18 ($i_w = 40^\circ$, $\delta_f = 60^\circ$, U_o = 18.6 ft/sec).

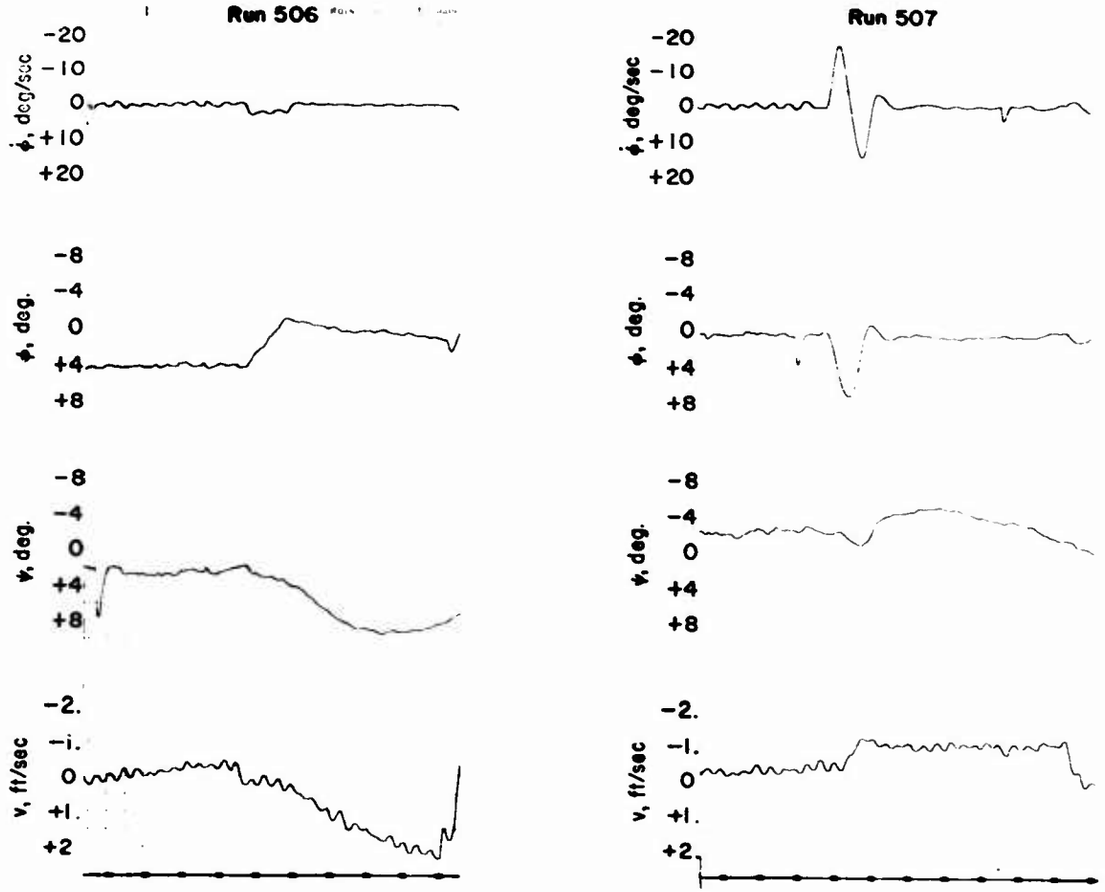

$K_\phi = 0$, $K_{\dot{\phi}} = 1$ f.s., $K_{\dot{\psi}} = 0$

Run 506

Gains 1/4 f.s., $K_{a\beta} = 0.18$

Run 507

Figure 29. Lateral-Directional XC-142 Model Responses at a Fixed Decelerating Condition ($i_w = 40^\circ$, $\delta_f = 60^\circ$, $U_o = 30$ ft/sec).

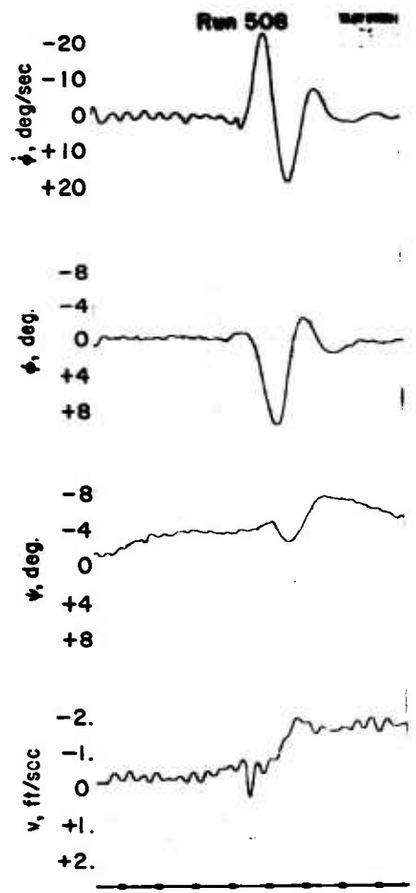

Gains -1/8 f.s., $K_{a\beta}$ = 0.18

Run 508

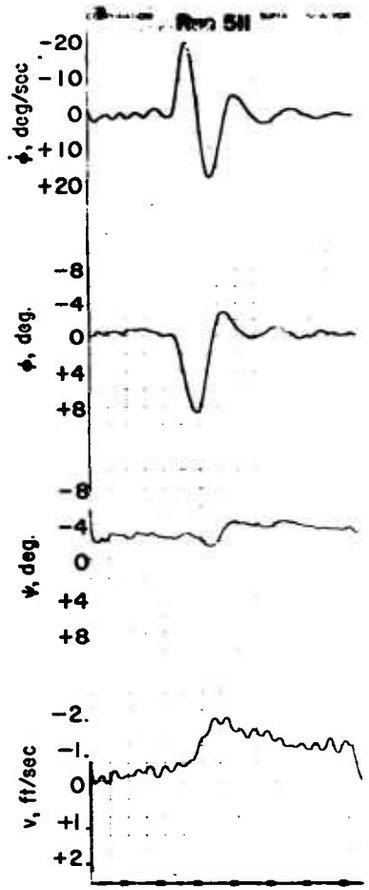

Gains -1/8 f.s., $K_{a\beta}$= 0.36

Run 511

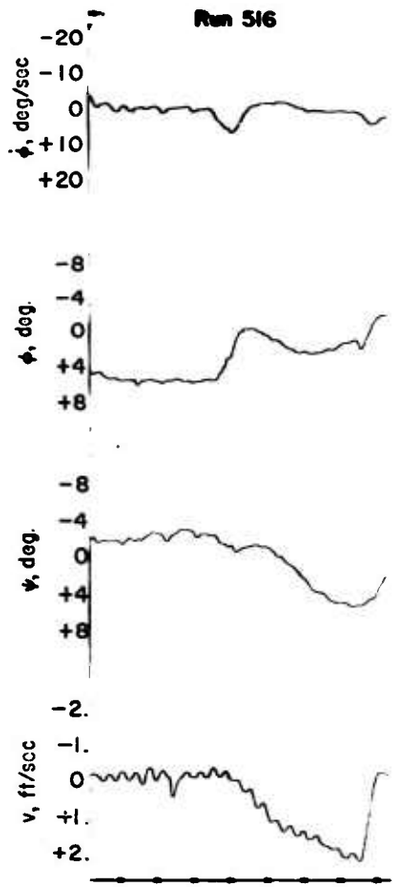

K_ϕ = 0, $K_{\dot{\phi}}$ -1/8 f.s. $K_{\dot{\psi}}$ = 1/8 f.s.

Run 516

Figure 29. Continued.

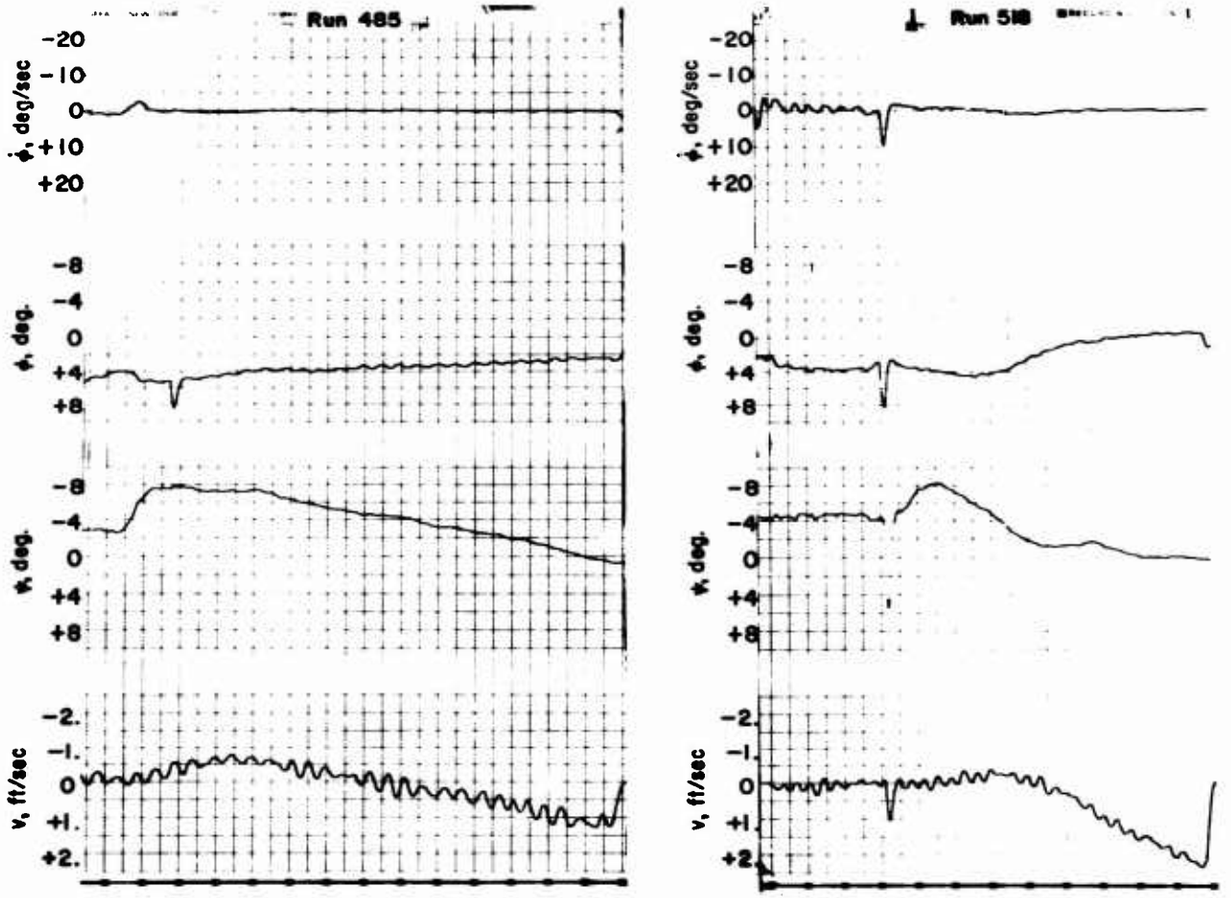

U_o = 18.6 ft/sec — Run 485

U_o = 30 ft/sec — Run 518

$K_\phi = 0$, $K_{\dot{\phi}}$ - 1/4 f.s., K_ψ - 1/8 f.s., $K_{a\beta} = 0.18$

Figure 30. Lateral-Directional XC-142 Model Responses to Aileron Inputs ($i_w = 40^\circ$, $\delta_f = 60^\circ$).

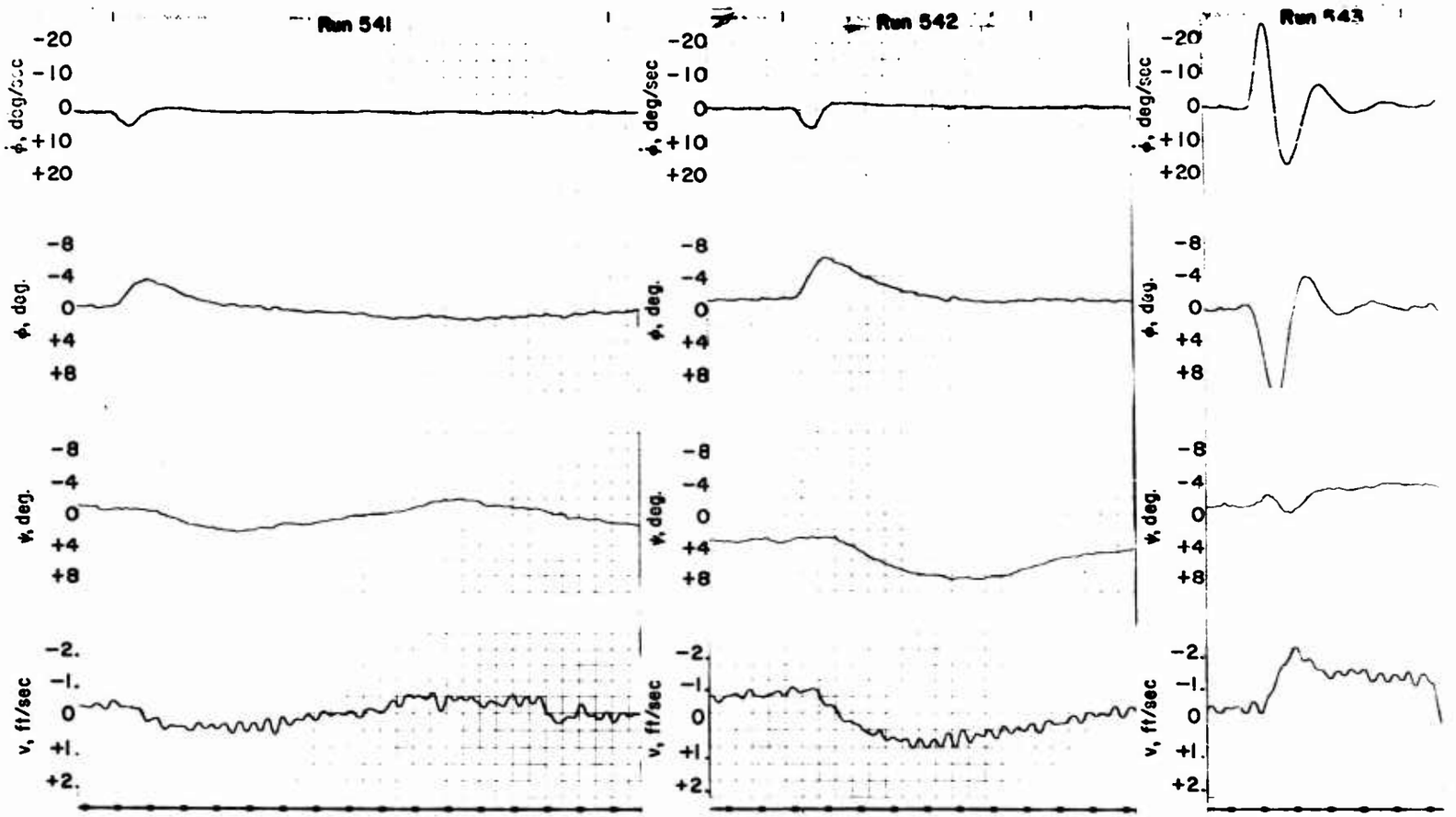

$K_{\dot{\psi}}$ - 1/8 f.s., $K_{\dot{\phi}}$ - 1/8 f.s.
Run 541

$K_{\dot{\psi}}$ - 1/8 f.s., $K_{\dot{\phi}}$ - 1/4 f.s.
Run 542

Gains 1/8 f.s., $K_{a\beta}$ = 0
Run 543

Figure 31. Lateral-Directional XC-142 Model Responses at Fixed Accelerating Condition ($i_w = 40^\circ$, $\delta_f = 60^\circ$, U_o = 15 ft/sec).

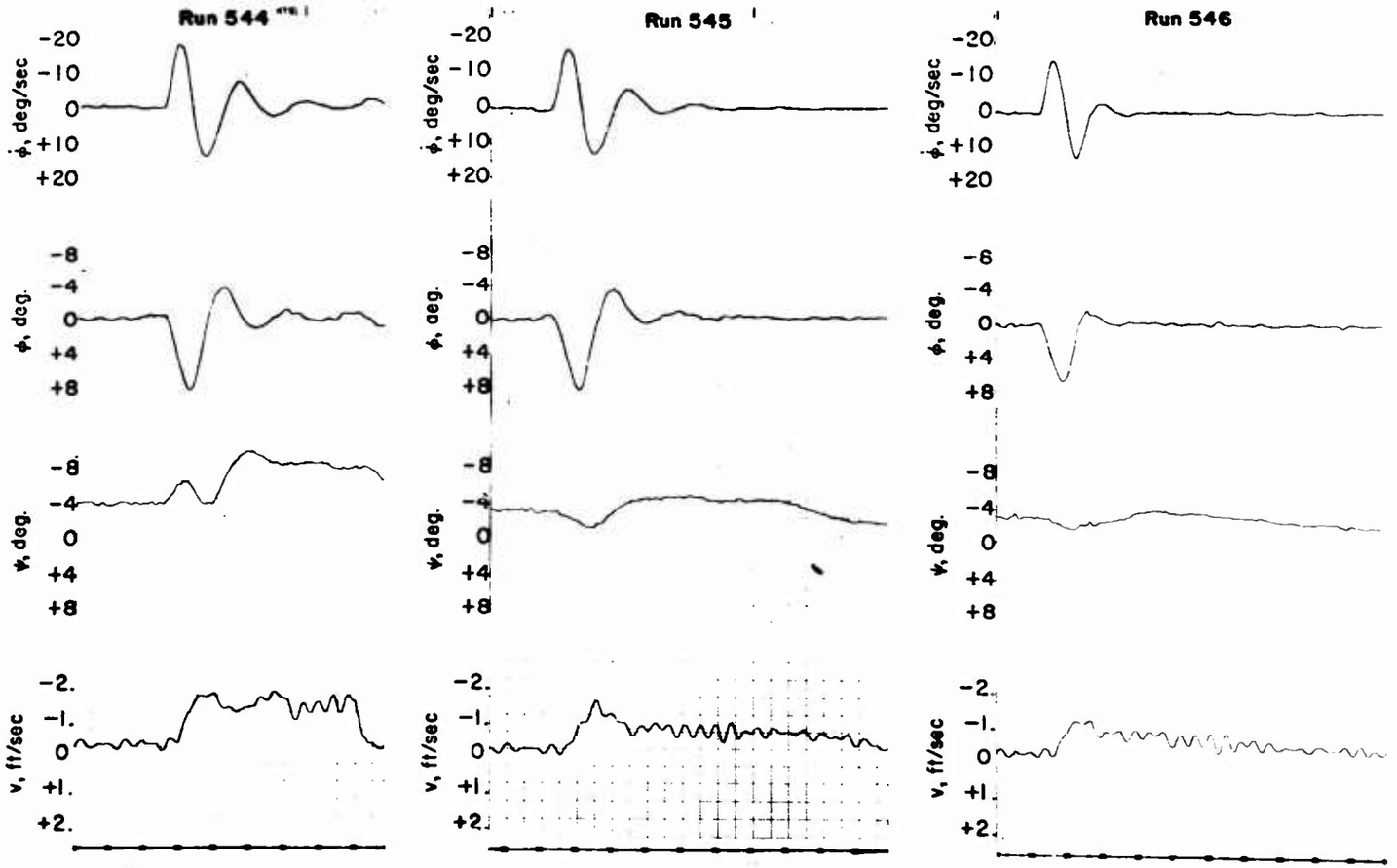

Gains 1/8 f.s., $K_{a\beta}$ = 0
Run 544

Gains 1/8 f.s., $K_{a\beta}$ = 0.18
Run 545

Gains 1/4 f.s., $K_{a\beta}$ = 0.18
Run 546

Figure 31. Continued.

LITERATURE CITED

1. T. A. Dukes, J. M. Carballal, P. M. Lion, Some Dynamic Aspects of Stability in Low-Speed Flying Machines, U. S. Army Transportation Research Command, Fort Eustis, Virginia, TRECOM Technical Report 63-56, November 1963.

2. D. McRuer, I. Ashkenas, D. Graham, Aircraft Dynamics and Automatic Control, Systems Technology, Inc., August 1968.

3. G. Beppu and H. C. Curtiss, Jr., An Analytical Study of Factors Influencing the Longitudinal Stability of Tilt-Wing VTOL Aircraft, U. S. Army Aviation Materiel Laboratories, Fort Eustis, Virginia, USAAVLABS Technical Report 66-53, July 1966, AD640945.

4. R. A. Curnutt and H. C. Curtiss, Jr., Comparison of Longitudinal Stability Characteristics of Three Tilt-Wing VTOL Aircraft Designs, U. S. Army Aviation Materiel Laboratories, Fort Eustis, Virginia, USAAVLABS Technical Report 66-64, September 1968, AD667983.

5. H. C. Curtiss, Jr., W. F. Putman, and J. V. Lebacqz, An Experimental Investigation of the Longitudinal Dynamic Stability Characteristics of a Four-Propeller Tilt-Wing VTOL Model, U. S. Army Aviation Materiel Laboratories, Fort Eustis, Virginia, USAAVLABS Technical Report 66-80, September 1967, AD663848.

6. E. Martinez, A New Facility for the Study of Aircraft Dynamics, U. S. Army Transportation Research Command, Fort Eustis, Virginia, Project No. 9-38-01-000, TK902, July 1961.

7. M. E. Shields, H. F. Stahl, and G. T. Upton, Estimated Flying Qualities, XC-142A V/STOL Assault Transport, Ling Temco Vought, Inc., Vought Aeronautics Division, Dallas, Texas, Report No. 2-53310/4R939, May 1964.

8. R. P. Boyden and H. C. Curtiss, Jr., Investigation of the Lateral/Directional Stability Characteristics of a Four-Propeller Tilt-Wing VTOL Model, U. S. Army Aviation Materiel Laboratories, Fort Eustis, Virginia, USAAVLABS Technical Report 68-19, April 1968, AD673147.

9. W. F. Putman, An Investigation of the Lateral/Directional Dynamic Stability Characteristics of a Tilt-Wing V/STOL Transport Model in Simulated Low-Speed Descending Flight, U. S. Army Aviation Materiel Laboratories, Fort Eustis, Virginia, USAAVLABS Technical Report 69-46, July 1969, AD859807.

Unclassified
Security Classification

DOCUMENT CONTROL DATA - R & D

(Security classification of title, body of abstract and indexing annotation must be entered when the overall report is classified)

1. ORIGINATING ACTIVITY (Corporate author) Department of Aerospace and Mechanical Sciences Princeton University Princeton, New Jersey	2a. REPORT SECURITY CLASSIFICATION Unclassified 2b. GROUP

3. REPORT TITLE

FEEDBACK CONTROL OF VTOL AIRCRAFT

4. DESCRIPTIVE NOTES (Type of report and inclusive dates)

Final Report

5. AUTHOR(S) (First name, middle initial, last name)

Theodor A. Dukes

6. REPORT DATE	7a. TOTAL NO. OF PAGES	7b. NO. OF REFS
April 1970	67	9

8a. CONTRACT OR GRANT NO. DA 44-177-AMC-47(T) b. PROJECT NO. Task 1F162204A14235 c. d.	9a. ORIGINATOR'S REPORT NUMBER(S) USAAVLABS Technical Report 69-96 9b. OTHER REPORT NO(S) (Any other numbers that may be assigned this report)

10. DISTRIBUTION STATEMENT

This document is subject to special export controls, and each transmittal to foreign governments or foreign nationals may be made only with prior approval of U. S. Army Aviation Materiel Laboratories, Fort Eustis, Virginia 23604.

11. SUPPLEMENTARY NOTES	12. SPONSORING MILITARY ACTIVITY
	U. S. Army Aviation Materiel Laboratories Fort Eustis, Virginia

13. ABSTRACT

The behavior of poles and zeros characterizing the longitudinal dynamics of VTOL aircraft in transition is analyzed and discussed. In feedback design, it is desirable to create a dominant attitude response mode which is separated in frequency and varies little throughout the transition. This investigation has demonstrated that this goal can be achieved at fixed operating points in transition without accurate prior knowledge about the behavior of the stability and control derivatives during transition. In the longitudinal degrees of freedom, pitch attitude and pitch rate feedback were used. In the lateral-directional degrees of freedom, the same goal was achieved by using yaw rate, roll angle, and roll rate feedback. The gains were determined by an approximate procedure. Longitudinal and lateral-directional experiments were performed with a 0.1 scale model of the XC-142A tilt-wing VTOL aircraft. Pulse responses of the free-flying model are presented. In the longitudinal tests, accelerating and decelerating transitions were flown with the loop closures provided by a small analog computer. The lateral-directional tests were conducted at mid-transition at a trim velocity of 18.6 ft/sec. Tests at speeds of 15 ft/sec and 30 ft/sec were conducted representing accelerating and decelerating fixed points in transition, respectively. In these tests, the cross-control gain from differential collective to ailerons was used as a parameter in addition to the feedback gains. The results indicate that a tight yaw rate loop closure makes artificial control uncoupling unnecessary. A pronounced destabilizing effect occurred in the decelerating condition. In the accelerating condition, a more stable spiral mode was apparent.

DD FORM 1 NOV 68 1473 REPLACES DD FORM 1473, 1 JAN 64, WHICH IS OBSOLETE FOR ARMY USE.

Unclassified
Security Classification

14. KEY WORDS	LINK A		LINK B		LINK C	
	ROLE	WT	ROLE	WT	ROLE	WT
VTOL Aircraft Feedback Control Transition Pitch Attitude Attitude Rate Lateral-Directional Feedback Loops						